Effects of non-tracking solar collector orientation on energy production: Photovoltaic systems

Tauno Toikka

Master's thesis
University of Jyväskylä, Department of Physics
Master's Degree Program in Renewable Energy
29.02.2012
Instructor: Jussi Maunuksela
Contact: tauno.toikka@solaropt.com

Preface

This study has been carried out in Master's Degree Programme in Renewable Energy at the University of Jyväskylä.

I would like to thank my supervisor Jussi Maunuksela, Ph.D. who gave me free hands to make my thesis in the way I felt it had to be done and still advised and helped me whenever there was a need. I am grateful to my girlfriend Iida Korenius who was supportive and helpful through the whole study process. I would also like to thank my friend physics student Janne Kauppinen of all the reasonable and constructive criticism.

Jyväskylä, January 2012
Tauno Toikka

Abstract

This Master's thesis proposes a new method for calculating the optimum tilt and orientation angle of a fitted solar collector. In addition to using geographical data, this method takes into account the radiation data and weather statistics of prospective locations. This makes the calculations valid not only for certain latitudes, but also for certain radiation and weather conditions.

Calculations were done by estimating the energy production of a given solar array using a sequence of different tilt angles and orientation angles. Special attention was given to shaded solar arrays and arrays made up of photovoltaic modules. Specific radiation and weather data was used for both locations. Also, the different attributes of different phovoltaic modules were taken into consideration.

The proposed method is illustrated with two examples. Two solar arrays in two different locations were chosen: one in Southern Finland in Helsinki (60.12^o N, 24.57^o E), and the other in Central Finland in Viitasaari (63.07^o N, 25.68^o E).

The calculations for the solar array in Helsinki, which is in planning stage, take into account the shading caused by row installation. Calculations were made for c-Si PV modules. The optimum tilt angle was calculated as 28.6^o and the optimum orientation as 0.1^o from south to west.

The array in Viitasaari is an existing one, and the calculated optimum tilt and orientation angles were compared to the actual angles used at the location. The solar collector used there is a semi-transparent a-Si PV module. The optimum tilt angle was calculated as 46.4^o, and the actual angle at the site was 5^o. The optimum orientation angle was calculated as 4.3^o from south to east, and angle used was 0^o, i.e. south.

Contents

1 Introduction

The need to investigate the issue of this thesis arose in another context. When making my Research exercise the answer about optimal tilt angle for fitted solar collector was needed. I personally found it hard to find the precise information about what is the optimal orientation and above all, what is the optimal tilt angle for fitted solar collectors from leading literatures and from scientific articles. If the answer was found about orientation then the typical answer was south, which is pretty reasonable. On the other hand the typical answer about tilt angle was in the form of $Latitude \pm 10^o$ or $Latitude - 20^o$ *to* $Latitude$. The most sophisticated answer was found from Luque [4]. In this reference the suggestion was a first degree function with one parameter, which was *Latitude*. In all suggestions the optimal tilt angle depended on only one parameter, which was *Latitude*.

It is obvious that latitude is not the only parameter that has effect on the optimum tilt angle. For example London (England) and Kiev (Ukraine) are pretty much in same latitude. London is a foggy place, and Kiev is a sunny place. Thus, in Kiev the greater percentage of radiation comes directly from the sun compared to London. As this was the case, collectors in Kiev should be oriented more towards to the sun compared to London. On the other hand, in London collectors should be directed more towards the sky dome. Thus, the optimum tilt angle for collectors in Kiev might be near latitude but in London the angle might be latitude minus some degrees.

In our modern world where everything needs to be optimized particularly in the sector of energy production, we might ask why the direction of solar collectors does not need to be optimized. Solid state physicists are doing a considerable amount of work to make our solar modules more and more effective, yet we place them on our roofs in more or less random directions.

In some sense it is understandable. Module makers need to sell modules and thus it is in their best interests to make them as good as possible. The middle man between module makers and consumers intends to sell modules, and this he will do with the module specifications. The final yield is not his main concern. When a module has been sold it is the clients task to optimize it. Typically, customers have no ability to estimate the optimum installation for their solar system. They rely on the seller's or the manufacturer's rough approximations, and in the end pay the price.

It is obvious that installing systems in the optimal direction does not require any more physical effort that installing it in some other direction. The only thing needed is adequate estimation and that is the focus of this thesis.

Case Helsinki Pitäjänmäki In this case, the sales manager from SunWind Gylling Oy contacted us. For a competitive bidding they needed tentative calculations about the optimum tilt angle and energy yield for a PV-power plant. The planned system is in the size scale of 140 kWp (biggest in Scandinavia) and it is planned to be located in Pitäjänmäki, Helsinki. The solar array is planned to contain 700 Swedmodule GPV200 solar modules [Appendix 2]. Preliminary requirements were 50 rows of modules with 14 modules in each row. The distance between the rows had a requirement of 3 m and an orientation of 20^o from south to west. The whole system is to be placed on rooftop supported by stands.

Near Pitäjänmäki lies Kumpula, where Finnish Meteorological Institute (FMI) [14] happens to have measurement station for solar radiation. The distance between these two locations is only between 4 to 5 km. For our calculations we assume radiation and weather conditions to be equal in Kumpula and Pitäjänmäki.

One year measurement data was received from FMI measured in Helsinki Kumpula for tentative calculations for Sunwind Gylling Oy. The three years measurement data was received later for the use of this thesis, because the measurement station has existed only for a while. Only round years were used as data because it is not reasonable to stress any particular season. The data for tentative calculations besides date and time included global and diffuse radiation for each hours of the year 2009. The Data from FMI used here also includes average ambient temperature and average wind speed for each hour during the years 2007-2009.

In addition to this, the data on the location of the solar system was necessary. The data on location can be found in table 1. Also, the necessary data on planned solar modules can be found in table 2.

Table 1: Essential data from Helsinki Kumpula (Radiation measurement station). Data is from [14].

Local Latitude (ϕ)	60.12^o
Local Longitude (LL)	24.57^o
Average starting time of thermal winter	26.12
Average ending time of thermal winter	30.03

Case Viitasaari Viitasaari is a small town in central Finland and which has a service station. The cafeteria of the service station has a terrace roof made of transparent PV-modules (fig. 1) [Appendix 3]. The size of the solar system is 4.2 kWp with a total of 154 ASITHRU-30-SG modules. The

Table 2: Essential data about solar modules planned to use in Helsinki Pitäjänmäki. All data are from manufacturer's data [Appendix 2]. Subscript STC stands for standard test conditions: 1000 W/m^2, 25^oC, 1.5 AM.

$V_{OC,STC}$	36.6 V
$V_{MPP,STC}$	29.0 V
$I_{SC,STC}$	7.58 A
$I_{MPP,STC}$	7.01 A
NOCT	46^oC
Temperature coefficient for voltage	$-0.0034/K$
Temperature coefficient for current	$0.00034/K$
Cell type	c-Si
Back surface of the module	Tedlar
Number of cells in module	60

tilt and orientation angles are 5^o and 0^o which are not optimums, but are defined by architectural points of departures. Our interest here is to discover the optimum tilt and orientation angles, and estimate how much has been lost with existing settings.

Figure 1: The terrace roof of the service station in Viitasaari [13].

University of Jyväskylä has a weather station in Viitasaari. The global radiation data, the ambient temperature data and the wind speed data have been collected during the years 2004-2009. Also, the energy yield of the solar array has been filed. In our calculations the data of the years 2004 and 2009 have been excluded because there is no data from complete years. Also,

the year 2005 has been excluded due to some confusion with time filing in the beginning of the year. Calculations were done using date, time, global radiation, average ambient temperature and average wind speed for each hour during the years 2006-2008. Also the information in tables 3 and 4 were used.

Table 3: Essential data about location of Viitasaari

Local Latitude (ϕ)	63.07^o
Local Longitude (LL)	25.86^o
Average starting time of thermal winter [14]	26.11
Average ending time of thermal winter [14]	20.04

Table 4: Essential data about solar modules used in Viitasaari [Appendix 3]. Subscript STC stands for standard test conditions: 1000 W/m^2, 25^oC, 1.5 AM.

$V_{OC,STC}$	49 V
$V_{MPP,STC}$	36 V
$I_{SC,STC}$	1.02 A
$I_{MPP,STC}$	0.75 A
NOCT	-
Temperature coefficient for voltage	$-0.0033/K$
Temperature coefficient for current	$0.0008/K$
Cell type	a-Si
Back surface of the module	Glass
Number of cells in module	-

The underlying pattern in this thesis is to calculate the radiation on a tilted surface as accurately as possible, to take into account the shading effect in a reasonable way and to do photovoltaic calculations using only the data that is typically available in the manufacture's data sheets. In the field of radiation we use the symbols from Ref. [3], in the field of shading effect we use symbols from Ref. [6] and in the field of photovoltaic generation we use symbols from Ref. [4]. List of the basic symbols used in this work can be found in Nomenclature in [Appendix 1].

Words radiation and irradiation here were not used randomly: radiation implies the amount of solar radiation in joules per square meter J/m^2 and irradiation implies to the power of illumination produced by radiation per square meter W/m^2. Illumination is our general way to express that radiation or irradiation occurs.

2 Definitions

2.1 Direct and diffuse sun light

Direct sunlight represents a beam which has not suffered scattering in the earth's atmosphere. Diffused sunlight has suffered scattering in the earth's atmosphere. Scattering can be caused by air, dust, aerosol, clouds, drops of water or ground (and all the obstacles the ground includes).

In this thesis we denote solar radiation as H. With the subscript b we denote direct solar radiation (H_b). With the subscript d we denote diffused solar radiation (H_d). H_b and H_d have been quantified the way that $H_d + H_b = H_g$, where H_g is global radiation [2].

2.2 Solar constant

Solar constant gives the average sun irradiation outside the earths atmosphere. In this thesis we use symbol G_{sc} for it. There are some variations in this constant in different literatures. For example in Duffie & Becham [3] G_{sc} is 1367 W/m^2 and in Meinel [2] G_{sc} is 1353 W/m^2. In this work we use $G_{sc} = 1367\ W/m^2$.

2.3 Declination

If we assume that the earths orbit forms a plane around the sun and the Earths rotation forms a rotation axis, then the angle between the axis and the plane varies from -23.45^o to 23.45^o during a year (see fig. 2). This variation angle is called declination and is denoted as δ. Declination can be calculated from the following equation [1]:

$$\delta = 23.45^o \sin\left(360^o \frac{284 + n}{365}\right) \tag{1}$$

where n is the number of a day of a year. For example for the eight day of February n=39 and $\delta = -15.52^o$.

2.4 Hour angle

The symbol ω is used for an hour angle. Hour angle describes earths rotation around its own axis. In one day the hour angle goes from -180^o to 180^o. For solar noon (=sun is in it's uppermost position) the hour angle has been chosen to be 0^o. In every one hour after the noon the hour angle increases 15 degrees and in every one hour before noon hour angle decreases 15 degrees.

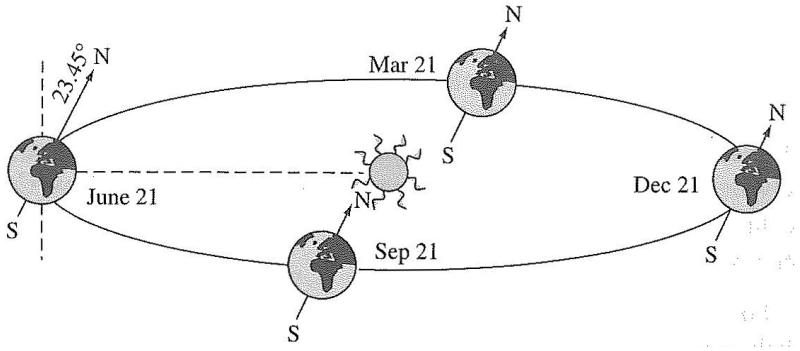

Figure 2: Earth's movement on its orbit plane that causes the declination [4].

That means for example that at 12:00 $\omega = 0^o$, at 13:00 $\omega = 15^o$, at 14:00 $\omega = 30^o$, at 11:00 $\omega = -15^o$, at 10:00 $\omega = -30^o$ and so on [1].

Solar time Solar time describes the dependence between the angular motion of the sun across the sky, the time we use and the location of the observer. It can expressed as

$$solar\ time = 15^o * (TO - AO - 12) + (LL - LH) \tag{2}$$

where LL is the local longitude and LH is the longitude of the local timezone, both of them in degrees [4](positive for east longitudes and negative for west longitudes). TO is the local official time and AO is the correction parameter, both in hours. Correction parameter is needed for example when clocks are set ahead by one hour in summer time. In that case $AO = 1$.

Equation of time There is a small variation in earth rotation that has not been included in the time that humans use. The variation is annual and it is in scale of $\pm 4^o$ ($\sim \pm 15\ min$). The variation is illustrated in figure 3.

Equation of time describes the variation and it can be expressed as

$$\begin{aligned} E = \frac{1}{4} 229.2^o (&0.000075 + 0.001868 \cos B - 0.032077 \sin B \\ &- 0.014615 \cos(2B) - 0.04089 \sin(2B)) \end{aligned} \tag{3}$$

where $B = (n-1)\dfrac{360^o}{365}$ and n is the number of a day of a year [3]. Thus the hour angle that conforms its definition is

$$\omega = solar\ time + E \tag{4}$$

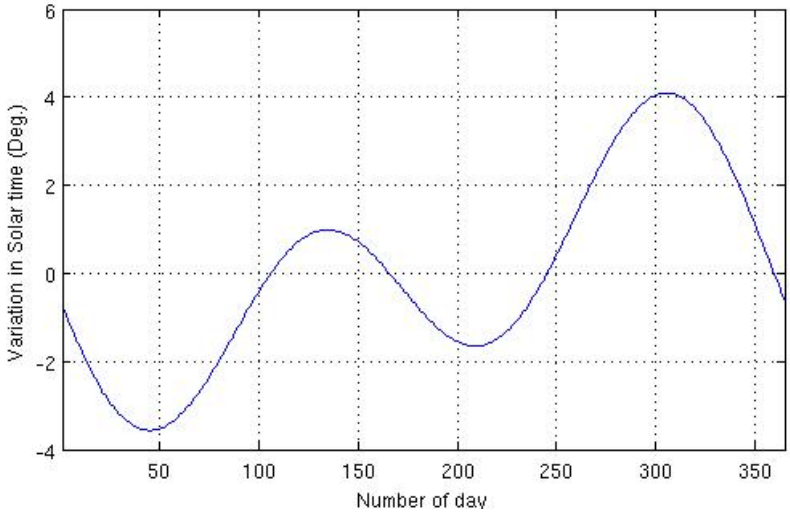

Figure 3: Variation in hour angle compared to solar time.

2.5 Zenith and profile angle from the position of the sun

In figure 4 there is illustrated horizontal surface and tilted surface. The angle that tilted surface is tilted compared to horizontal surface is β. The orientation of tilted surface is γ and it is zero in south, positive from south to west and negative from south to east. Zenith is the normal of the horizontal surface. The angle between the direction of beam radiation and zenith is called zenith angle θ_z and the angle between the direction of beam radiation and horizontal surface is called solar altitude angle α_s.

The angle of incidence is the angle between the direction of beam radiation and the normal of tilted surface. It is denoted as θ. The angle of incidence is related to tilt and orientation angle in a way that can be described with equation

$$\begin{aligned}\cos\theta = &\sin\delta\sin\phi\cos\beta - \sin\delta\cos\phi\sin\beta\cos\gamma + \cos\delta\cos\phi\cos\beta\cos\omega \\ &+ \cos\delta\sin\phi\sin\beta\cos\gamma\cos\omega + \cos\delta\sin\beta\sin\gamma\sin\omega\end{aligned} \tag{5}$$

where ω is the hour angle, δ is the declination and ϕ is the local latitude [3].

For horizontal surfaces $\beta = 0$. That means that for horizontal surfaces from equation 5 only first and third terms remains. Thus we get relation between zenith angle for horizontal surface with other angles as:

$$\cos\theta_z = \cos\phi\cos\delta\cos\omega + \sin\phi\sin\delta \tag{6}$$

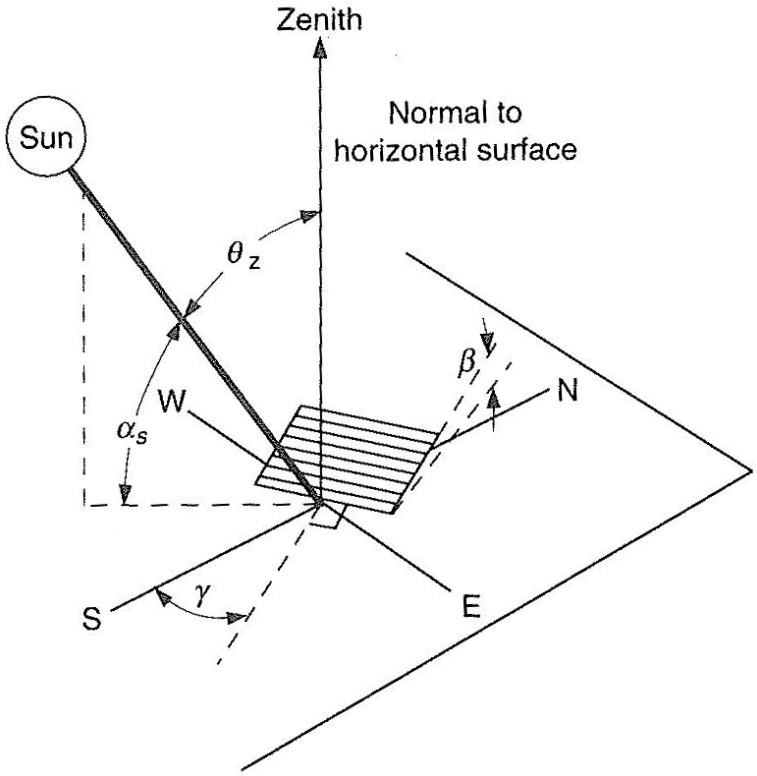

Figure 4: Horizontal surface, tilted surface, the sun, zenith angle as θ_z, surface tilt angle as β, surface slope/orientation angle as γ and solar altitude angle as α_s [3].

In figure 5 there is illustrated profile angle α_p which is also an essential angle. Other angles in figure 5 are the same as in the figure 4. Profile angle is related to other angles of figures 4 and 5 in the following way:

$$\tan \alpha_p = \frac{\tan \alpha_s}{\cos(\gamma_s - \gamma)} \tag{7}$$

where γ_s is the solar azimuth angle and in equation form

$$\gamma_s = \text{sign}(\omega) \left| \cos^{-1} \left(\frac{\cos \theta_z \sin \phi - \sin \delta}{\sin \theta_z \cos \phi} \right) \right| \tag{8}$$

and α_s solar altitude angle and as figure 4 demonstrates $\alpha_s = 90^o - \theta_z$.

2.6 Air Mass

Air mass AM is the unitless measure of the relative path length of solar radiation through the atmosphere. It has been defined to be one when solar

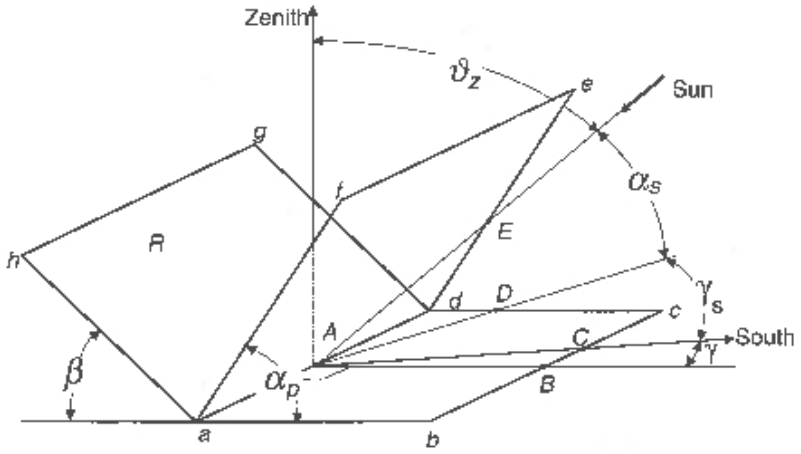

Figure 5: Profile angle α_p and some other essential angles related to tilted surface R and the suns position [3].

radiation goes vertically through the atmosphere at sea level. That means that $AM = 1$ when sun is at zenith. AM increases when the solar zenith angle increases. An approximative expression for air mass is as follows [3]:

$$AM = \frac{1}{\cos \theta_z} \tag{9}$$

According to this equation AM goes infinite when $\theta_z \rightarrow 90^o$. This is an unphysical situation and we can expect that equation 9 gives inaccurate values when the sun is near the horizon. On the other hand irradiation levels at these moments are low. Thus also the effect of inaccurate AM is low when calculating overall radiation.

2.7 Ground reflectance

Ground reflects light and when solar collector is tilted some of that light will end on solar collector. Ground reflectance can be quantified as the relative amount of light that ground reflects.

Ground reflectance is denoted as ρ. It is a fraction between reflected radiation to total radiation. Thus it is ranged between 0 and 1 in the way that 0 means no reflected radiation at all and 1 means that all radiation reflects.

If there is no information available about the magnitude of ground reflectance, using $\rho = 0.2$ for approximation is recommended [2], [3]. It is a good approximation for most cases, but significant variation in the ground

reflectance exists when the ground is cowered with snow. A good average estimation for snow covered ground is $\rho = 0.7$ [2], [3].

3 Radiation on horizontal surface

3.1 Extraterrestrial radiation on a horizontal surface

The average extraterrestrial irradiation is defined by solar constant which is 1367 W/m^2. However, it varies during a year because of the variation of the distance between the earth and the sun. The variation of the extraterrestrial irradiation is about $\pm 3\%$ during a year [2].

Extraterrestrial irradiation can be expressed as a function of a day of a year with the following equation [3]

$$G_{on} = G_{sc}\left(1 + 0.033\cos\frac{360^o n}{365}\right) \tag{10}$$

where G_{sc} is solar constant and n is the number of a day of a year.

For horizontal surface equation 10 is

$$G_o = G_{sc}\left(1 + 0.033\cos\frac{360^o n}{365}\right)\cos\theta_z \tag{11}$$

This can be considered as irradiation on earth's surface without the atmosphere. Using equation 6 in equation 11 we get

$$G_o = G_{sc}\left(1 + 0.033\cos\frac{360n}{365}\right)(\cos\phi\cos\delta\cos\omega + \sin\phi\sin\delta) \tag{12}$$

In some cases we need to know extraterrestrial radiation on horizontal surface at certain period of time in a day. An equation for those cases can be achieved by integrating the equation 12 over ω. Integration gives us

$$\begin{aligned} H_0 = \frac{12 * 3600}{\pi} G_{sc}\left(1 + 0.033\cos\frac{360^o n}{365}\right)\Bigg[\cos\phi\cos\delta(\sin\omega_2 - \sin\omega_1) \\ + \frac{\pi(\omega_2 - \omega_1)}{180}\sin\phi\sin\delta\Bigg] \end{aligned} \tag{13}$$

where ω_1 and ω_2 are limits of time in form of hour angles so that $\omega_1 < \omega_2$ [3]. This equation gives the extraterrestrial radiation on horizontal surface between times ω_1 and ω_2.

3.2 Clearness index

In general there are two types of radiation data available. In most cases the data of solar radiation is in the form of global radiation. Global radiation

means total radiation on a horizontal surface. Some solar radiation measurement stations can give global and diffuse radiation components separately. When there is only global radiation data available estimation of diffuse radiation component needs to be done. A key for estimating the diffuse radiation is so called clearness index. Clearness index has been defined as

$$k_T = \frac{H_g}{H_0} \tag{14}$$

where H_g is total radiation on horizontal surface and H_o is extraterrestrial radiation [3].

Correlation between clearness index k_T and H_d/H_g has been found in hourly repeated measurements. Figure 6 illustrates the type of data that has been measured. This type of data has been received from many studies. The

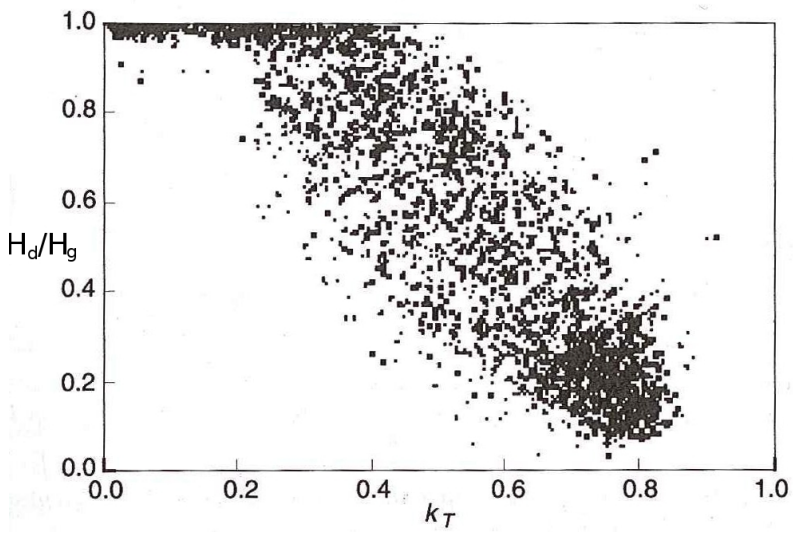

Figure 6: Measured correlation between clearness index and diffuse radiation divided by total radiation [3].

curve fittings from three different studies are shown in figure 7.

In this thesis we use the curve fitting by Erbs et al. [10] from figure 7. The analytical expression for this curve is

$$\frac{H_d}{H_g} = \begin{cases} 1.0 - 0.09k_T & \text{for } k_T \leqslant 0.22 \\ 0.9511 - 0.1604k_T + 4.388k_T^2 & \\ -16.0638k_T^3 + 12.366k_T^4 & \text{for } 0.22 < k_T \leqslant 0.80 \\ 0.165 & \text{for } k_T > 0.80 \end{cases} \tag{15}$$

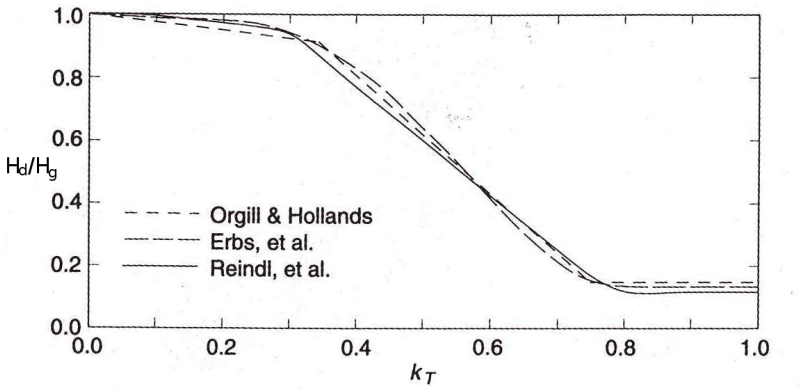

Figure 7: Curve fitting from three different measurements illustrating the correlation between k_T and H_d/H_g [3].

4 Radiation on tilted surface

Typical type of radiation data available is the data of radiation on horizontal surface. On the other hand, horizontal plane is not the plane where highest annual radiation occurs (equator is an exception). Thus, we need to find a method to estimate the radiation on tilted surface based on the radiation data on horizontal surface. The following sections will present some of these methods.

4.1 Ratio between beam radiation on horizontal surface to beam radiation on tilted surface

When transformation from radiation on horizontal surface to radiation on tilted surface needs to be done, we need ratio between beam radiation on tilted surface to beam radiation on horizontal surface. This ratio is denoted in this thesis as R_b:

$$R_b = \frac{\text{Beam radiation on tilted surface}}{\text{Beam radiation on horizontal surface}} \tag{16}$$

Using equations 5 and 6 it can be written as

$$R_b = \frac{H_b * \cos\theta}{H_b * \cos\theta_z} \tag{17}$$

where H_b is a direct beam radiation [3]. Thus

$$R_b = \frac{\cos\theta}{\cos\theta_z}. \tag{18}$$

The term $\cos\theta$ gives negative values when radiation incidences on back surface of solar collector. When we assume that radiation on back surface is not exploitable then

$$R_b = \frac{\min(0, \cos\theta)}{\cos\theta_z} \tag{19}$$

In equation 19 there is $\cos\theta_z$ in denominator. The term $\cos\theta_z \longrightarrow 0$ when $\theta_z \longrightarrow 90^o$. This happens when the sun is rising or setting down. In these cases R_b can have unrealistically high values because of the low denominator in equation 19. In hourly calculations for those hours, during which the sun is rising or setting down, reference [3] suggests to use equation:

$$R_{b.ave} = \frac{\int_{\omega_i}^{\omega_{ii}} \cos\theta \ d\omega}{\int_{\omega_i}^{\omega_{ii}} \cos\theta_z \ d\omega} = \frac{A}{B} \tag{20}$$

where

$$\begin{aligned} A = {} & (\sin\delta \sin\phi \cos\beta - \sin\delta \cos\phi \sin\beta \cos\gamma)\frac{\pi}{180}(\omega_{ii} - \omega_i) \\ & + (\cos\delta \cos\phi \cos\beta + \cos\delta \sin\phi \sin\beta \cos\gamma)(\sin\omega_{ii} - \sin\omega_i) \\ & - (\cos\delta \sin\beta \sin\gamma)(\cos\omega_{ii} - \cos\omega_i) \end{aligned} \tag{21}$$

and

$$B = (\cos\phi \cos\delta)(\sin\omega_{ii} - \sin\omega_i) + (\sin\phi \sin\delta)\frac{\pi}{180}(\omega_{ii} - \omega_i) \tag{22}$$

In noon ω_i is the hour angle of the starting point of the hour under examination and ω_{ii} is the sunset hour angle. In morning ω_i is the sunrise hour angle, that is -(sunset hour angle), and ω_{ii} is the ending point of the hour under examination. Sunset hour angle ω_s can be found from equation:

$$\cos\omega_s = -\tan\phi \tan\delta \tag{23}$$

4.2 Radiation components

To make radiation calculations on tilted surface possible we need to split total radiation into components. Beam and diffuse radiation occur on tilted surface. Theoretically, light reflected from ground does not end up on horizontal surface but it does end up on tilted surface. Thus, general way to express radiation on tilted surface in three components is

$$H_T = H_{T,b} + H_{T,d} + H_{T,r} \tag{24}$$

where $H_{T,r}$ is radiation reflected from ground [4].

4.3 Isotropic sky

Isotropic sky assumption is a simple way to calculate all three radiation components ($H_{T,b}$, $H_{T,d}$, $H_{T,r}$) on tilted surface. The main idea of it is that it assumes diffuse radiation coming equally from all directions of skydome [3]. For tilted surface the relative visible part of the skydome to the surface can be expressed as $(1 + \cos\beta)/2$ where β is tilt angle of the surface.

Also, ground reflection is assumed to be homogeneous from all directions. It means that the amount of irradiation you receive is constant regardless of the direction you look at the ground.

The relative visible part of ground for a tilted surface can be expressed as $(1 - \cos\beta)/2$. Thus equation 24 becomes for isotropic sky as

$$H_T = H_b R_b + H_d \left(\frac{1 + \cos\beta}{2} \right) + H_g \rho \left(\frac{1 - \cos\beta}{2} \right) \tag{25}$$

4.4 Anisotropic sky

In isotropic sky assumption we assumed diffuse radiation coming equally from all directions of the skydome. It is a good approximation, but true only for heavily overcast skies. Figure 8 illustrates diffuse radiation distribution over skydome in a real case. In figure 8 the isotropic sky case would be a straight horizontal line representing diffuse radiation distribution. From figure 8 it can be found that the highest diffuse radiation occurs from skydome near to the sun. It can be easily seen by eye when examining the sky. Also, the diffuse radiation near the horizon can be higher than elsewhere. This shows as a small mound at 80^o zenith angle in figure 8.

In anisotropic sky assumption we examine the diffuse radiations in components. We assume there to be three types of diffuse radiation: isotropic diffuse which comes from equally all directions of skydome, circumsolar diffuse which comes from small area around the sun and diffuse from the horizon. Also, beam radiation and ground reflected radiation are included in. The components are illustrated in figure 9.

4.4.1 Perez model

There are few ways to estimate anisotropic sky. Some of them are presented in [3] and [4]. References [3], [4] and [6] suggest that the best of them is the so-called Perez model [8]. Perez model is the most accurate in taking account the different sky conditions. On the other hand, it is also the most complex one.

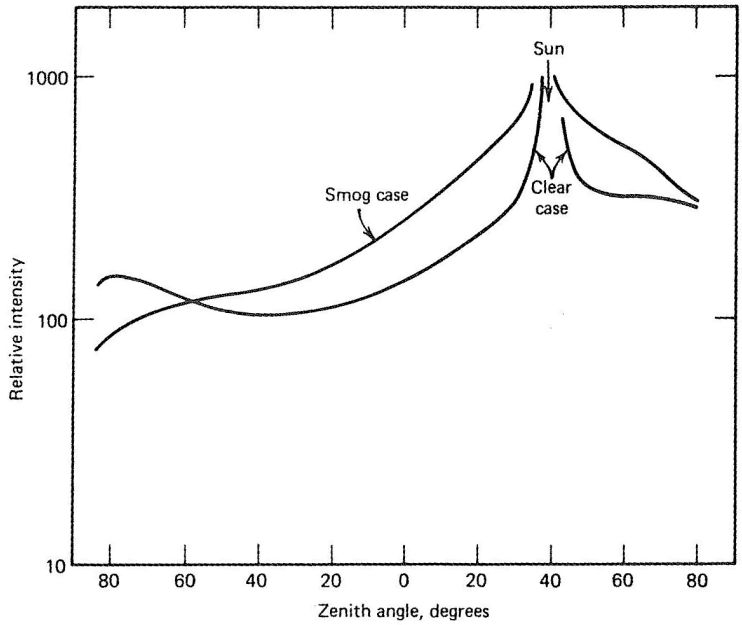

Figure 8: Distribution of diffuse radiation with different zenith angles [3].

Different sky conditions are defined through clearness ε so that

$$\varepsilon = \frac{\frac{H_d + H_d * \sin^{-1}\beta}{H_d} + 5.535 * 10^{-6}\theta_z^3}{1 + 5.535 * 10^{-6}\theta_z^3} \tag{26}$$

where H_d is a diffuse radiation to the horizontal surface, θ_z is a zenith angle and β is a tilt angle.

Using clearness ε we can calculate circumsolar brightening coefficient F_1 and horizontal brightening coefficient F_2 so that

$$F_1 = \max\left[0, f_{11} + f_{12}\Delta + \frac{\pi\theta_z}{180}f_{13}\right] \tag{27}$$

and

$$F_2 = f_{21} + f_{22}\Delta + \frac{\pi\theta_z}{180}f_{23} \tag{28}$$

Empirically adjusted parameters f_{11}, f_{12}, f_{13}, f_{21}, f_{22} and f_{23} are functions of ε and they can be found in table 5.

Also, other versions of table 5 exist. For example, reference [3] uses clearness table from 1988. The table used in this thesis is from 1990 and was the latest to be found and for that reason was chosen to be used here. The fact that Quaschning [6] presented this table encouraged to use this version.

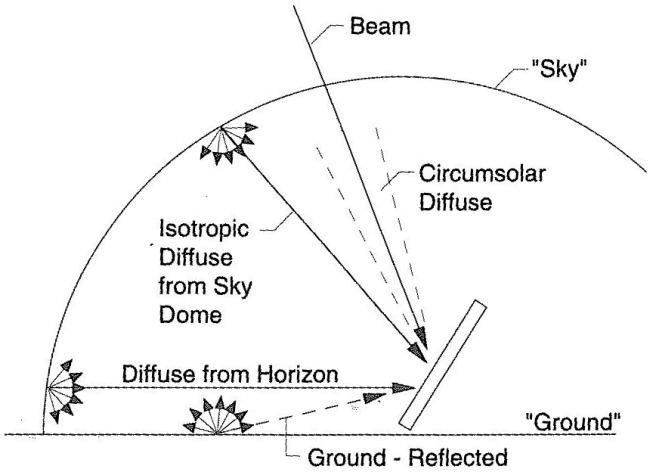

Figure 9: Radiation components in anisotropic sky assumption [3].

Table 5: Parameters for calculating brightening coefficients [8].

ε class	range of ε	f_{11}	f_{12}	f_{13}	f_{21}	f_{22}	f_{23}
1	1.000 - 1.065	-0.008	0.588	-0.062	-0.060	0.072	-0.022
2	1.065 - 1.230	0.130	0.683	-0.151	-0.019	0.066	-0.029
3	1.230 - 1.500	0.330	0.487	-0.221	0.055	-0.064	-0.026
4	1.500 - 1.950	0.568	0.187	-0.295	0.109	-0.152	-0.014
5	1.950 - 2.800	0.873	-0.392	-0.362	0.226	-0.462	0.001
6	2.800 - 4.500	1.132	-1.237	-0.412	0.288	-0.823	0.056
7	4.500 - 6.200	1.060	-1.600	-0.359	0.264	-1.127	0.131
8	6.200 - ∞	0.687	-0.372	0.250	0.156	-1.377	0.251

Parameter Δ in equations 27 and 28 is the atmospheric brightness which is defined as

$$\Delta = AM \frac{H_d}{H_{on}} \tag{29}$$

where AM is the air mass, H_d is the diffuse radiation and H_{on} the extraterrestrial normal incidence radiation which can be found from equation 10.

The diffuse radiation component to tilted surface according to Perez model can be written as

$$H_{d,T} = H_d \left[(1 - F_1) \left(\frac{1 + \cos\beta}{2} \right) + F_1 \frac{a}{b} + F_2 \sin\beta \right] \tag{30}$$

where

$$a = \max[0, \cos\theta] \tag{31}$$

and

$$b = \max[\cos 85, \cos \theta_z] \tag{32}$$

Note that $\frac{a}{b}$ is most of the time same as R_b.

Now total radiation on tilted surface according to Perez model is

$$\begin{aligned} H_T = H_b R_b + H_d(1 - F_1)\left(\frac{1 + \cos\beta}{2}\right) + H_d F_1 \frac{a}{b} \\ + H_d F_2 \sin\beta + H_g \rho \left(\frac{1 - \cos\beta}{2}\right) \end{aligned} \tag{33}$$

It is worth to note that the first term in this equation represents direct beam radiation, the second term represents isotropic diffuse, the third term represents circumsolar diffuse, the fourth term represents diffuse from horizon and the fifth term represents radiation reflected from ground. To make it easier to refer the components of the function 33 in future we denote the equation 33 as

$$H_T = H_{T,b} + H_{T,d,iso} + H_{T,d,cs} + H_{T,d,hz} + H_{T,r} \tag{34}$$

5 Self shading

One of the most common shading problems in solar collector systems is so-called self shading. By self shading we mean solar collectors that are in rows, that are tilted and are partly shading each others. Figure 10 illustrates this type of installation.

Figure 10: Example of row installed solar array [16]

According to figure 10 we can expect the shading problems to occur for beam radiation component to tilted surface when the sun is near to the horizon. Also we can expect that the part of the skydome the solar collector sees is restricted by the collector row in front of it. That will reduce the diffuse radiation component. We can also expect that the radiation reflected from the ground between the solar collectors is neglectible.

We can eliminate these kind of shading problems by installing solar collectors on horizontal plane. Figure 11 illustrates this type of installation. However, we do not recommend this practice. Furthermore, we will note that higher irradiation will be received when the surface is tilted, even if self shading occurs and also for PV - systems higher energy yields will be received by tilting the PV - modules. Also, not tilting the solar collectors will cause higher losses by increased dirt and snow coverage effects.

Geometrical solution Figure 12 will lead us to a geometrical solution of the self shading problem. We will examine this situation in two dimensions which is a cross-section of rows (see fig. 12). The two dimensional model is used because we assume that radiation from the ends of the rows is neglectible. There are three explanations for the assumption.

Figure 11: Example of an solar array installed on a horizontal plane. Linköping's public library in Sweden [Appendix 2].

Firstly, if solar collectors are properly fitted they are facing south or near south. This means that direct and circumsolar diffuse end up on solar collectors when the sun is rising or setting down (see fig. 13). When the sun is setting down it is near the horizon and radiation is going through to the high air mass. This leads to low radiation levels during those moments.

Secondly, when radiation is coming from the side of the collector, the angle of incidence θ is high (near to 90^o). Increasing angle of incidence causes the decrease of irradiation.

Third and the most remarkable point is the fact that basically all solar collectors are covered by glass (PV - systems and solar heat collectors). It is a law of optics that beam of light does not pass the glass at high inclination angles. Figure 14 gives an example of this.

We can also explain our assumption from another point of view. When the rows are long and the relative distances between the rows are small, we can assume the rows to be infinitely long. When the rows are infinitely long then there is no radiation from the ends of the rows. This leads us to a situation where two dimensional examination is acceptable. Now on we call this assumption as the long row assumption.

In the next chapters we will examine shading effects for all five radiation components from equation 34 separately.

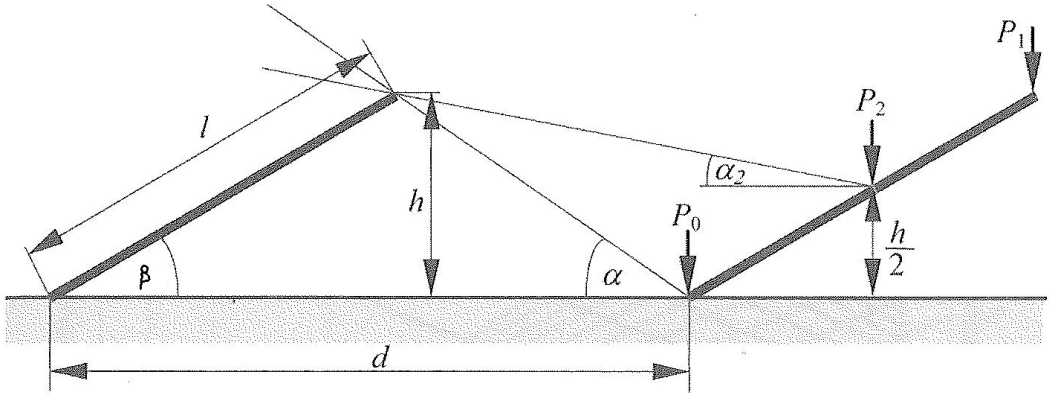

Figure 12: Geometrical illustration of angles and dimensions we use here [6].

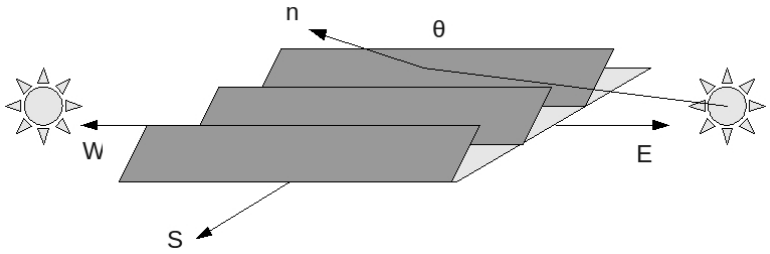

Figure 13: Illustration of sun position with respect to a properly orientated solar array when sun is raising or setting down.

5.1 Beam radiation component

Point P_1 on solar collector in figure 12 does not suffer any shading effect. At the moment when the sun rises above horizon, point P_1 is almost immediately illuminated. When sun keeps rising, direct beam radiation starts reaching lower and lower points from solar collector until it reaches to the point of P_0. During that period of time the amount of radiation that ends up on solar collector is about the same as if only the area between P_1 and P_2 would be under illumination. In both cases the irradiation is the same. On the other hand, irradiation is also the same when the whole solar collector is under illumination half of the time of the period.

In case of some solar collectors like solar heat collectors we can use point P_2 as a reference point. That means the whole solar collector is illuminated by beam radiation when sun rises above angle of α_2. The case is equally the same as when the sun is setting down. Beam radiation stops on solar collector when the sun has been set down under the angle of α_2. Generalizing this, beam radiation reaches on solar collector when profile angle α_p is greater

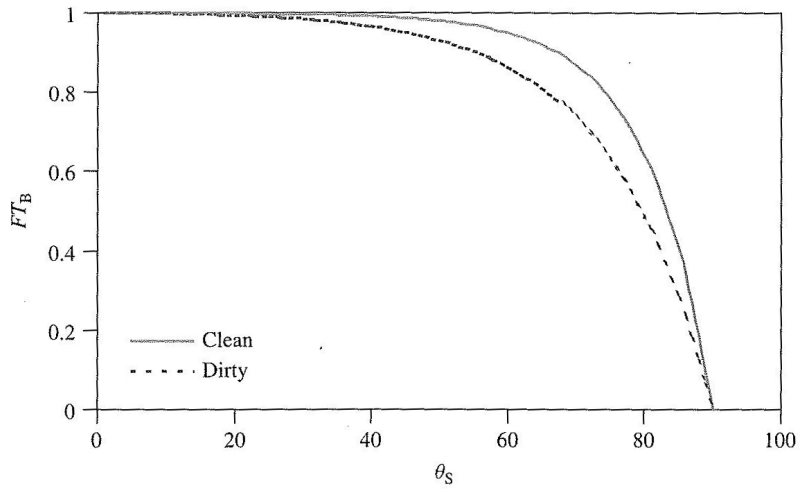

Figure 14: Effect of angle of incidence against relative transmittance of glass cover [4]

than α_2 (see fig 5 and 12).

In case of solar heat collector we can use above assumption. However, there is a issue with Photovolatic systems. General fact is that partly shaded PV - panel acts poorly [6]. Typical solar panels are formed from solar cells. To get adequate voltage several cells in series are installed, typically the number of cells is about 36 [6]. When one cell in a module has been partly shaded remarkable reduction of whole module power has been detected. Reference [6] suggest that when only one cell of the 36 cell module is shaded only partly (75%), the decrease of module power can be 70%. This means shading module by 2% decreases module power by 70%. The explanation for this is shaded cell in series of cells acts like a load. One cell acting as a load drops module current and thus whole module power.

There is a solution for this sort of problem and the solution is a bypass diode. When a cell or cells connected behind a bypass diode start acting as a load, current starts to go through the diode. Figure 15 illustrates module I - V characteristics when different amount of bypass diodes are installed and when one cell of the modules of the 36 cells is shaded.

Only when there is a bypass diode for every cell the module loses part of the power that is almost equal to the part that is lost by shading.

Typically there is one bypass diode for 18-24 cells and almost all solar modules have only two bypass diodes [6]. This leads to poor acting of module under shading conditions. When we look at figure 12 we can say that no shading effect(for beam radiation) occurs when solar altitude angle is above α. Thus, we suggest that for the modules with two or less bypass diodes

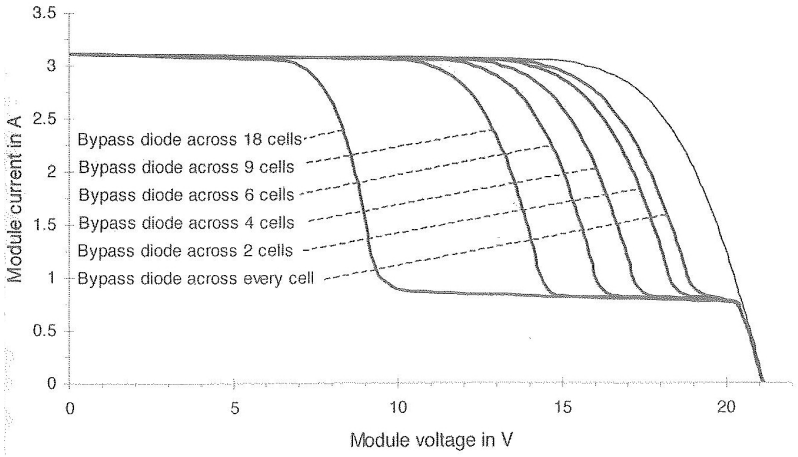

Figure 15: I - V characteristic for partly shaded PV - solar cell with different amount of bypass diodes [6].

should use P_0 as a reference point. Reference [6] suggests to do this for all PV-systems. Reference point P_2 could be considered when there is a bypass diode for every cell in the module.

In practice the angles α and α_2 from figure 12 are needed for handling the shading problem. Using symbols from figure 12 the angles are

$$\alpha = \arctan\left(\frac{u \sin\beta}{1 - u\cos\beta}\right) \tag{35}$$

and

$$\alpha_2 = \arctan\left(\frac{u \sin\beta}{2 - u\cos\beta}\right) \tag{36}$$

where

$$u = \frac{l}{d} \tag{37}$$

[6]. The problem can be solved by assuming that beam radiation on solar collector occurs when profile angle α_p (from equation 7) is higher than α_2 in general case and α in case of Photovolatic system. Thus, beam radiation on tilted surface under shading effect is

$$H_{T,b,sh} = H_{T,b} * \mathrm{SE_b} \tag{38}$$

where shading effect on beam radiation component $\mathrm{SE_b}$ is defined as

$$\mathrm{SE_b} = \begin{cases} 1 & \text{when } \alpha_p > \alpha \\ 0 & \text{when } \alpha_p \leqslant \alpha \end{cases} \tag{39}$$

5.2 Isotropic diffuse radiation component

There is no shading effect on isotropic diffuse radiation component. When the sun is above horizon isotropic diffuse radiation always occurs on all areas of solar collector. Thus, there is no need to separate PV - systems from other solar collectors.

Row installation causes another type of effect. When we examine figure 12 it can be noticed that the area on skydome point P_0 sees is limited by the row in front of it. If we use the long row assumption, what the area point P_0 sees, is illustrated in figure 16.

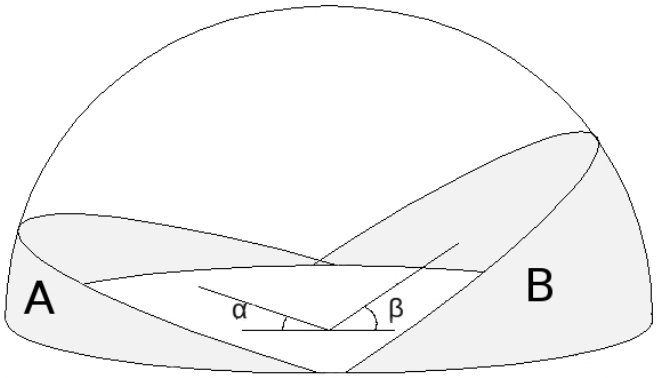

Figure 16: Illustration of skydome and the part that tilted and shaded solar collectors in long row sees.

Diffuse radiation from area B (fig. 16) is out of tilted solar collectors range even if no shading effect occurs. Areas A and B (fig. 16) of the isotropic sky can not be seen from point P_0 (fig. 12). From the average point P_2 (fig. 12) can not be seen area $\frac{1}{2}A + B$ (fig.16) of the isotropic sky. We use the point P_2 (fig.12) as a reference point. Point P_2 sees from isotropic skydome the area that can be expressed as $(1+\cos(\beta+\alpha_2))/2$. That is relative area when whole sky is defined to be one. Thus isotropic diffuse radiation component under above mentioned shading conditions based on equation 33 is

$$H_{T,d,iso,sh} = H_d(1 - F_1)\left(\frac{1 + \cos(\beta + \alpha_2)}{2}\right) \tag{40}$$

5.3 Circumsolar diffuse radiation component

We treat shading effect on circumsolar diffuse radiation component pretty much the same as we treat shading effect on beam radiation component. Only exception is that we use P_2 (fig. 12) as a reference point also for PV -

systems as we did for solar collectors in sec 5.1. Point P_2 is used because it is the average point on solar collector as it was explained in section 5.1. Also, it should be noted that in a real situation when the sun is above the horizon circumsolar diffuse always ends up on whole area of solar collector. In our mathematical approach we assume circumsolar diffuse coming from the same direction as beam radiation and for that reason it seems that circumsolar diffuse end up on whole solar collector when sun's altitude angle is higher than α. In a real case circumsolar diffuse comes from the area around the sun and the intensity of it decreases when going further from the sun on skydome.

Thus, solution for shading effect on circumsolar diffuse is: circumsolar diffuse occurs on solar collector when profile angle α_p is higher than α_2 from figure 12. Thus, circumsolar radiation on tilted surface under shading effect is

$$H_{T,d,cs,sh} = H_{T,d,cs} * \mathrm{SE_{cs}} \tag{41}$$

where shading effect on circumsolar diffuse radiation component $\mathrm{SE_{cs}}$ is defined as

$$\mathrm{SE_{cs}} = \begin{cases} 1 & \text{when } \alpha_p > \alpha_2 \\ 0 & \text{when } \alpha_p \leqslant \alpha_2 \end{cases} \tag{42}$$

5.4 Horizontal diffuse radiation component

Because horizontal diffuse radiation comes from the horizon the row of collectors in front of a solar collector blocks the diffuse radiation when we use long row assumption. Thus horizontal diffuse radiation ends up only on the first row of solar collectors. We suggest to use a factor 1/N, where N is number of rows, to correlate the lack of horizontal diffuse radiation on the rows behind the first one. This gives to the horizontal diffuse radiation component (from equation 33) a form of

$$H_{T,d,hz,sh} = \frac{1}{N} H_{T,d,hz} = H_d \frac{1}{N} F_2 \sin\beta \tag{43}$$

5.5 Ground reflected radiation component

It is obvious that for the first row of solar collectors ground reflection occurs in a normal way. For other rows there is not much of the ground reflect because a row in front of it shadows the ground. Effect of ground reflecting on tilted surface is in general case neglectible [4]. Effect on rows behind the first one is much smaller. Thus, the rows behind the first one could be considered dropping out entirely of the examination. Assuming the ground

reflecting only for the first row, based on equation 33 we get ground reflected radiation on tilted surface under shading conditions as

$$H_{T,r,sh} = H_g \frac{1}{N} \rho \left(\frac{1 - \cos \beta}{2} \right) \tag{44}$$

where N is the number of rows.

5.6 Total radiation on tilted surface under shading effect

The total radiation on tilted surface when self shading effect occurs can now be summarized into one equation:

$$\begin{aligned} H_{T,sh} = {} & H_b R_b \mathrm{SE_b} + H_d (1 - F_1) \left(\frac{1 + \cos(\beta + \alpha_2)}{2} \right) + H_d F_1 \frac{a}{b} \mathrm{SE_{cs}} \\ & + H_d \frac{1}{N} F_2 \sin \beta + H_g \frac{1}{N} \rho \left(\frac{1 - \cos \beta}{2} \right) \end{aligned} \tag{45}$$

For simplicity in future, different terms in previous equation are expressed as

$$H_{T,sh} = H_{T,b,sh} + H_{T,d,iso,sh} + H_{T,d,cs,sh} + H_{T,d,hz,sh} + H_{T,r,sh} \tag{46}$$

6 Effect of glass cover and dust

This far we have been pointing out the calculation methods to calculate radiation on some surface. The surface could be a plank of wood, a plasma television or a solar collector. In case of solar collectors we must bring out a really important point: almost all solar collectors, whether they are PV - cells or solar heat collectors, are covered by glass or some other material of this type. The amount of radiation which passes the glass is strongly dependent on the angle of incidence (see fig 14). Effect of the angle of incidence to the relative transmittance can be expressed as

$$FT(\theta) = 1 - b_0\left(\frac{1}{\cos\theta} - 1\right) \tag{47}$$

where FT is the relative transmittance so that FT for normal orientated beam ($\theta = 0$) is 1, θ is angle of incidence and b_0 is a constant that is related to the characteristics of the surface of the solar collector [4]. When b_0 is a unknown then general value $b_0 = 0.07$ can be used [4].

Also dust has an effect on transmittance of solar collectors surface and it is really realistic to assume that a solar collector which is on use is covered with dust. Dust has two kind of effects on transmittance: The other effect is relative to the degree of dirtiness of solar collector and the another effect depends on dirtiness level of solar collector and angle of incidence.

Parameter degree of dirtiness can be expressed as

$$T_{dirt}(0)/T_{clean}(0) = \frac{\text{Transmittance of dirt surface}}{\text{Transmittance of clean surface}} \tag{48}$$

where zero stands for $\theta = 0$. Thus $T_{dirt}(0)$ is a normal orientated transmittance for a dirt surface and $T_{clean}(0)$ is a normal orientated transmittance for a clean surface. Some classifications for the degree of dirtiness can be found from table 6.

Table 6: Empirically adjusted parameters to take into account the effect of glass cover and dust [4].

Dirtiness	$T_{dirt}(0)/T_{clean}(0)$	a_r	c_r
Clean	1	0.17	-0.069
Low	0.98	0.20	-0.054
Medium	0.97	0.21	-0.049
High	0.92	0.27	-0.023

Degree of dirtiness and angle of incidence effect on relative transmittance of surface of solar collector can be expressed for beam radiation component

as

$$\mathrm{FT_b} = 1 - \frac{\exp\left(-\frac{\cos\theta}{a_r}\right) - \exp\left(-\frac{1}{a_r}\right)}{1 - \exp\left(-\frac{1}{a_r}\right)} \tag{49}$$

where parameter a_r is related to degree of dirtiness and can be found in table 6. Because we assume circumsolar diffuse radiation component coming from the same direction as the beam radiation component, we use equation 49 also for estimating dirtiness and glass cover effect on circumsolar radiation component. Thus $\mathrm{FT_{cs}} = \mathrm{FT_b}$.

For isotropic diffuse radiation component relative transmittance can be expressed as

$$\begin{aligned} FT_d = 1 - \exp\Bigg[-\frac{1}{a_r}\Bigg[\frac{4}{3\pi}\left(\sin\beta + \frac{\pi - \beta\frac{\pi}{180} - \sin\beta}{1+\cos\beta}\right) \\ + c_r\left(\sin\beta + \frac{\pi - \beta\frac{\pi}{180} - \sin\beta}{1+\cos\beta}\right)^2\Bigg]\Bigg] \end{aligned} \tag{50}$$

and for ground reflected radiation component relative transmittance can be expressed as

$$\begin{aligned} \mathrm{FT_r} = 1 - \exp\Bigg[-\frac{1}{a_r}\Bigg[\frac{4}{3\pi}\left(\sin\beta + \frac{\beta\frac{\pi}{180} - \sin\beta}{1-\cos\beta}\right) \\ + c_r\left(\sin\beta + \frac{\beta\frac{\pi}{180} - \sin\beta}{1-\cos\beta}\right)^2\Bigg]\Bigg] \end{aligned} \tag{51}$$

where dirtiness level related constants a_r and c_r can be found from table 6.

Equations 49, 50 and 51 are from reference [11]. Unfortunately, relative transmittance for horizontal diffuse radiation component was not suggested. Our suggestion for upper limit for relative transmittance for horizontal diffuse radiation is to modify the equation 49 so that

$$\mathrm{FT_{hz}}(max) = 1 - \frac{\exp\left(-\frac{\cos(90-\beta)}{a_r}\right) - \exp\left(-\frac{1}{a_r}\right)}{1 - \exp\left(-\frac{1}{a_r}\right)} \tag{52}$$

The equation is in the above form because horizontal diffuse radiation is parallel with horizon and thus the smallest angle of incidence it can come

across with tilted surface is $90^o - \beta$. Considering the neglectible role of $H_{d,hz}$ in H_T we suggest that $\mathrm{FT_{hz}}(max) \approx \mathrm{FT_{hz}}$.

Now the total radiation on tilted surface taking account the effect of glass cover and dust is

$$\begin{aligned} H_{T,FT} = \frac{T_{dirt}(0)}{T_{clean}(0)}(H_{T,b}\mathrm{FT_b} + H_{T,d,iso}FT_d + H_{T,d,cs}\mathrm{FT_{cs}} \\ + H_{T,d,hz}\mathrm{FT_{hz}} + H_{T,r}\mathrm{FT_r}) \end{aligned} \tag{53}$$

For simplicity in future we label components from previous equation with following subscripts

$$H_{T,FT} = H_{T,b,FT} + H_{T,d,iso,FT} + H_{T,d,cs,FT} + H_{T,d,hz,FT} + H_{T,r,FT} \tag{54}$$

7 Photovoltaic generation

So far we have got the tools to calculate irradiation on tilted surface and irradiation on a solar collector, which has been covered by glass and dust. With these tools we can calculate optimum tilt and orientation angle for solar collector in general. In case of photovoltaic systems the ability of PV-system to transfer radiation into electricity needs to be taken into account. In following sections we present methods for that.

7.1 One diode equivalent circuit model

Solar cells have p-n-junction and it can be considered as a kind of diode. When there is no radiation on a solar cell it can be described as a diode. Electrical behavior of solar cell, which is under illumination conditions, can be described with the circuit in fig 17 [6]. Current I_{Ph} is so called photo current and it is dependent on radiation.

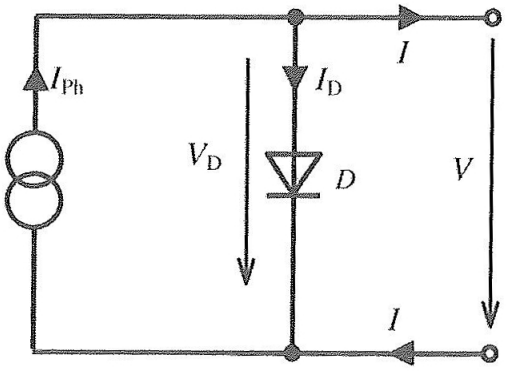

Figure 17: One diode circuit equivalent solar cell that is under illumination [6]

In practical case charge carriers suffer a voltage drop through the p-n-junction of a semiconductor. The voltage drop can be described with the series resistance R_s in figure 18 . Also, there is a small current leak involved in edges of the solar cell. That can be described with parallel resistance R_p in figure 18.

Using Kirchhoff's first rule on figure 18 circuit we get

$$0 = I_{Ph} - I_D - I_P - I \tag{55}$$

Using symbols from figure 18 diode current I_D can be expressed as $I_D = I_S(\exp(V_D/mV_t) - 1)$ where I_S is the diode's saturation current, m is the

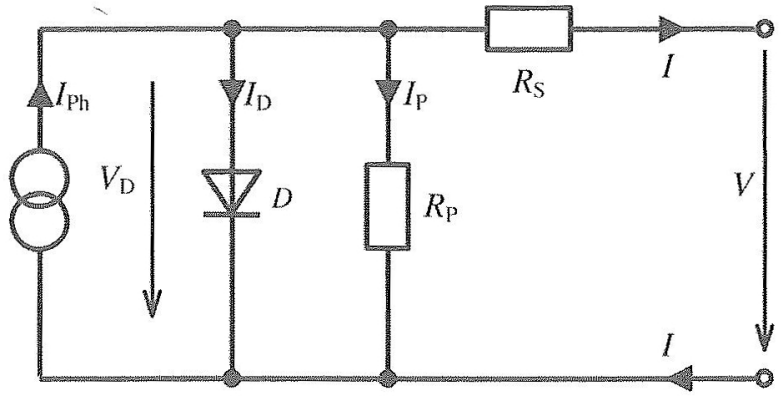

Figure 18: One diode equivalent circuit with parallel and series resistances [6].

diode factor and V_t is the thermal voltage [6] which can be calculated using equation $V_t = kT/e$, where k is the Boltzmann constant, e is the elementary charge and T is temperature in Kelvins [4]. It can be seen from figure 18 that the parallel current can be expressed as $I_P = V_D/R_P$ and $V_D = V + IR_S$. Thus the equation 55 comes out in a form of

$$0 = I_{Ph} - I_S\left(\exp\left(\frac{V + IR_S}{mV_t}\right) - 1\right) - \frac{V + IR_S}{R_P} - I \tag{56}$$

This equation is a general form that describes pretty well electrical behavior of a solar cell. Unfortunately, it is a little troublesome to use because of it's implicit form and in practice iteration methods are needed for solving it.

Parallel resistance can not be solved using only the data typically presented in manufacture's data sheet. On the other hand, we know that parallel resistance is relatively high (size scale of ohms) compared to series resistance (size scale of milliohms) [6]. Thus, the effect of parallel current is negligible [4].

We also know that photo current is approximately equal to short circuit current, $I_{SC} \approx I_{Ph}$ [4], [6].

These assumptions will give to equation 56 a form of

$$I = I_{SC} - I_S\left(\exp\left(\frac{V + IR_S}{mV_t}\right) - 1\right) \tag{57}$$

When cell's current is zero, cell is operating under open circuit condition. Thus, we get open circuit voltage from equation 57 so that

$$V_{OC} = mV_t \ln\left(\frac{I_{SC}}{I_S} + 1\right) \tag{58}$$

Solving saturation current from equation 58 we get

$$I_S = \frac{I_{SC}}{\exp\left(\frac{V_{OC}}{mV_T}\right) - 1} \tag{59}$$

Adding equation 59 in equation 57 we get

$$I = I_{SC} - I_{SC}\frac{\exp\left(\frac{V + IR_S}{mV_t}\right) - 1}{\exp\left(\frac{V_{OC}}{mV_T}\right) - 1} \approx I_{SC}\left[1 - \exp\left(\frac{V + IR_S - V_{OC}}{mV_t}\right)\right] \tag{60}$$

Constant m in equation 60 is a diode factor. Here we use as a diode factor the *ideal diode factor* that is $m = 1$. That is adequate for describing the I-V behavior of solar cell even if it slightly overestimates the I and the V [4]. This being the case

$$I = I_{SC}\left[1 - \exp\left(\frac{V + IR_S - V_{OC}}{V_t}\right)\right] \tag{61}$$

This equation describes I-V behavior of a solar cell [4]. Comparing to equation 56 the equation 61 is still implicit and thus cumbersome to use but on the other hand all parameters in it can be approximated using information of solar cells from manufacturer data sheet and information about radiation and weather conditions [4].

In many cases solar cell's open circuit voltage V_{OC}, short circuit current I_{OC}, operation voltage at the maximum power point V_{MPP} and operation current at the maximum power point I_{MPP} are given under standard test conditions (STC) by manufacture's data sheet. Series resistance R_S is temperature dependent but its temperature dependence is neglectible [6]. Reference [4] suggest that R_S is unaffected by the operation conditions. Thus we can estimate R_S from equation 61 in all radiation and weather conditions to be

$$R_S = \frac{V_{OC,STC} - V_{M,STC} + V_t \ln\left(1 - \frac{I_{M,STC}}{I_{SC,STC}}\right)}{I_{M,STC}} \tag{62}$$

where subscript STC refers to data at standard test conditions, which can be found from manufacture's data sheet. Thermal voltage V_t can be found by using $(273.15 + 25)\ K$ as a temperature T which is temperature under standard test conditions.

To define I-V characteristics of solar cells using equation 61, the parameters V_{OC} and I_{SC} are also needed. Methods to find them under real operation conditions are presented in the following sections.

7.2 Short circuit current I_{SC} under real operation conditions

Short circuit current is dependent on cell temperature. Increase in cell temperature causes increase in short circuit current. Dependence can be expressed with temperature coefficient value for current α_I which usually can be found from manufacture's data sheet. The temperature dependence for current ($\mathrm{TD_I}$) can be expressed with following equation

$$\mathrm{TD_I} = 1 + \alpha_I(T_c - T_{STC}) \tag{63}$$

where T_c is a cell temperature and T_{STC} is the temperature at standard test conditions, that is 25^oC [6]. Typical value-range for α_I is between $10^{-3}/^oC$ and $10^{-4}/^oC$.

Short circuit current is also dependent on irradiation. The dependence is linear as figure 19 demonstrates.

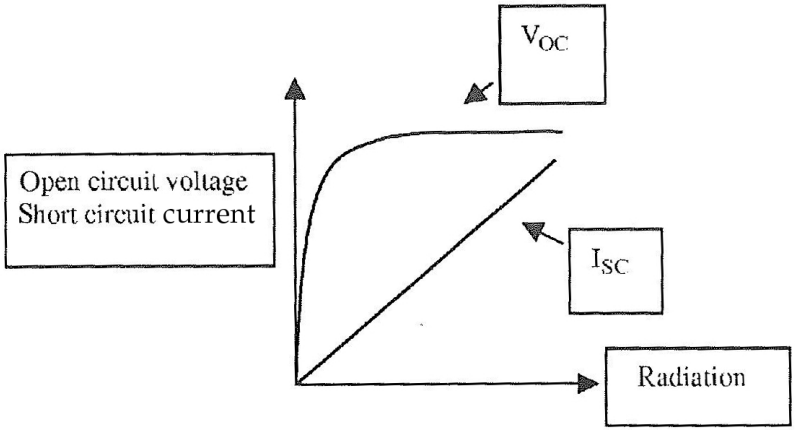

Figure 19: Typical I_{SC} and V_{OC} response of a solar cell against radiation [5].

With adequate accuracy linear dependence can be expressed as

$$I_{SC} = I_{SC,STC}\left(\frac{G_{eff}}{G_{STC}}\right) \tag{64}$$

where G_{eff} is effective irradiation on solar array, G_{STC} is irradiation at standard test conditions, that is 1000 W/m^2 and $I_{SC,STC}$ short circuit current at standard test conditions, that can be found from manufacturers data sheet [9].

In reference [12] is a presentation that takes into account the effect of solar cell's spectral response in short circuit current. In this presentation

G_{eff} from equation 64 can be replaced with the following equation

$$G_{eff} = G_b f_b + G_d f_d + G_r f_r \tag{65}$$

where f_b, f_d and f_r can be found from equation

$$f_i = c_i \exp[a_i(k_T - 0.74) + b_i(AM - 1.5)] \tag{66}$$

Empirically adjusted parameters a, b and c take into account the different irradiation components. For monocrystalline solar cell the parameters can be found from table 7, for polycrystalline solar cell the parameters can be found from table 8 and for amorphous silicon solar cells the parameters can be found from table 9.

Table 7: Empirical factors to estimate spectral response of a monocrystalline solar cell [12].

	H_b	H_d	H_r
a	$-3.13 * 10^{-1}$	$-8.82 * 10^{-1}$	$-2.44 * 10^{-1}$
b	$5.24 * 10^{-3}$	$-2.04 * 10^{-2}$	$1.29 * 10^{-3}$
c	1.029	0.764	0.970

Table 8: Empirical factors to estimate spectral response of a polycrystalline solar cell [12].

	H_b	H_d	H_r
a	$-3.11 * 10^{-1}$	$-9.29 * 10^{-1}$	$-2.70 * 10^{-1}$
b	$6.26 * 10^{-3}$	$-1.92 * 10^{-2}$	$1.58 * 10^{-2}$
c	1.029	0.764	0.970

Table 9: Empirical factors to estimate spectral response of a amorphous silicon solar cell [12].

	H_b	H_d	H_r
a	$-2.22 * 10^{-1}$	$-7.28 * 10^{-1}$	$-2.19 * 10^{-1}$
b	$9.20 * 10^{-3}$	$-1.83 * 10^{-2}$	$1.79 * 10^{-2}$
c	1.024	0.840	0.989

Summarizing the temperature effect and the spectral effect in equation 64 we get

$$I_{SC} = I_{SC,STC}[1 + \alpha_I(T_c - T_{STC})]\left(\frac{G_b f_b + G_d f_d + G_r f_r}{G_{STC}}\right) \tag{67}$$

7.3 Open circuit voltage under real operation conditions

Open circuit voltage is temperature dependent. Increase in cell's temperature causes a decrease in cell's open circuit voltage. The temperature dependency ($\mathrm{TD_V}$) can be expressed as

$$\mathrm{TD_V} = 1 + \alpha_V(T_c - T_{STC}) \tag{68}$$

where α_V is temperature coefficient for voltage and T_{STC} is the temperature at standard test conditions, that is 25^oC [6]. The temperature coefficient α_V can be found from manufacturer's data sheet. Typical value-range for α_V in case of silicon solar cell is between $-3 * 10^{-3}/^oC$ and $-5 * 10^3/^oC$ [6].

Irradiation level has also effect on open circuit voltage. It seems that higher irradiation causes higher open circuit voltage. Unlike in case of the short circuit current the dependence is not linear. Using the equation 64 and by making the assumptions that $I_{SC,STC}/I_S \gg 1$, we can derive from equation 58 irradiation effect on open circuit voltage. The derivation has been done in reference [9] and the result is

$$V_{OC} = V_{OC,STC} + mV_t \ln\left(\frac{G_{eff}}{G_{STC}}\right) \tag{69}$$

where G_{eff} is an effective irradiation. This logarithmic dependence of irradiation is derived from equations based on one diode equivalent circuit model. Even though one diode model is the best we can have if we want to use input data only from the manufacture's data site, its weakness is solar cells behavior under low irradiation conditions. References [4] and [9] report that irradiation level dropping under 200 W/m^2 can cause significant drop in open circuit voltage.

At low irradiation conditions recombination rate in p-n junction starts to play a significant role [9]. If photo-current drops near to the recombination current, the open circuit voltage suffers a significant drop. Figure 19 illustrates the open circuit voltage behavior at different irradiation levels. One diode model does not take into account the open circuit voltage drop at low irradiation levels.

Reference [9] suggest to add second logarithmic term in equation 69 to fix the low irradiation behavior problem in one diode model. Unfortunately, the logarithmic term includes two parameters which need to be found out empirically. In essence of this study we can not use the term. Reference [4] and reference therein [18] suggest a similar type of two-logarithmic term that also includes two unknown parameters which need to be found out

empirically. In this case generally adequate values for these parameters were given and for that reason we use the two-logarithm term in this thesis. This being the case, irradiation level has an effect (IE) on open circuit voltage that can be described as

$$\mathrm{IE} = \left[1 + \rho_{OC} \ln\left(\frac{G_{eff}}{G_{OC}}\right) \ln\left(\frac{G_{eff}}{G_{STC}}\right)\right] \tag{70}$$

where G_{eff} is effective irradiation on solar collector and empirically adjusted parameters ρ_{OC} and G_{OC} can be approximated to be as -0.04 and G_{STC} respectively. Figure 20 illustrates the relative effect on open circuit voltage with respect of irradiation.

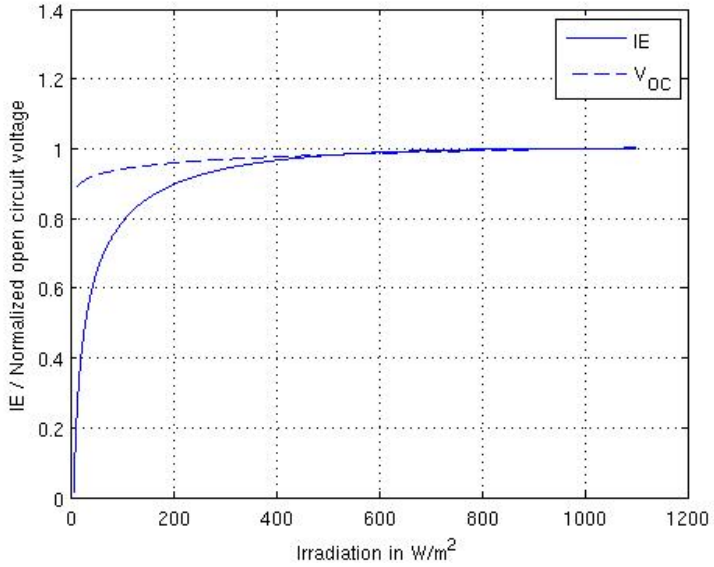

Figure 20: Effect of irradiation on normalized open circuit voltage in case of equation 69 using $m = 1$ (upper curvature) and in case of equation 70 (lower curvature).

Now we have the tools to calculate open circuit voltage dependence by using temperature and irradiation. The equation is

$$\begin{aligned} V_{OC} &= V_{OC,STC} * \mathrm{TD_V} * \mathrm{IE} \\ &= V_{OC,STC}[1 + \alpha_V(T_c - T_{STC})]\left[1 + \rho_{OC}\left[\ln\left(\frac{G_{eff}}{G_{STC}}\right)\right]^2\right] \end{aligned} \tag{71}$$

where $V_{OC,STC}$ is solar modules open circuit voltage at standard test conditions which can be found from manufactures data sheet.

7.4 Cell temperature

Information about cell temperature is needed for calculating short circuit current I_{SC}, open circuit voltage V_{OC} and thermal voltage V_t. Some methods for finding cell temperature are presented next.

7.4.1 Using NOCT

Ambient temperature and irradiation have effect on cell temperature. The effect can be described with following equation

$$T_{c,NOCT} = T_a + C_t G_{eff} \tag{72}$$

where $T_{c,NOCT}$ is the cell temperature, T_a is the ambient temperature, G_{eff} is the effective irradiation on surface and constant C_t is

$$C_t = \frac{NOCT(^oC) - 20}{800 W/m^2} \tag{73}$$

where $NOCT$ is normal operating cell temperature and generally can be found from manufacturer's data sheet [4]. Typical value is in range of 42^oC to 46^oC. When $NOCT$ is unknown approximation $C_t = 0.030^oC/(W/m^2)$ is reasonable [4]. When using NOCT value from manufacturer's data sheet it is expected that air can flow from the front and the back side of the solar module. If only partial flow from back side is allowed, NOCT can rise 17^oC and if back side is fully restricted from airflow, like in the case of some roof installations, NOCT can rise 35^oC.

7.4.2 Using wind speed

Wind speed has also effect on cell temperature. Luque et al. [4] referring to Ref. [19] suggest that it can be expressed as

$$T_{c,wind} = T_m + \frac{G_{eff}}{G_{STC}} \triangle T \tag{74}$$

where T_m is back surface temperature of solar module and can be expressed as

$$T_m = T_a + \frac{G_{eff}}{G_{STC}} [T_1 \exp(b * u_S) + T_2] \tag{75}$$

where u_S is the wind speed. Empirically adjusted parameters $\triangle T$, T_1, T_2, and b can be found from table 10.

Table 10: Empirically adjusted parameters for calculating effect of windspeed on cell temperature [4].

Type	$T_1(^oC)$	$T_2(^oC)$	b	$\triangle T(^oC)$
Glass/cell/glass	25.0	8.2	-0.112	2
Glass/cell/tedlar	19.6	11.6	-0.223	3

7.5 Power generated

Figure 21 illustrates typical V-I behavior of a solar cell. When voltage is zero solar cell operates at its maximum current, that is I_{SC}. When current is zero solar cell operates at its maximum voltage, that is V_{OC}. Short circuit current I_{SC} and open circuit voltage V_{OC} varies depending on the type and the quality of the solar cell and also by the aspects mentioned in sections 7.2 and 7.3. Solar cell's parallel resistance R_P and series resistance R_S have effect on curvature sharpness but shape of the curvature is pretty much standard [6].

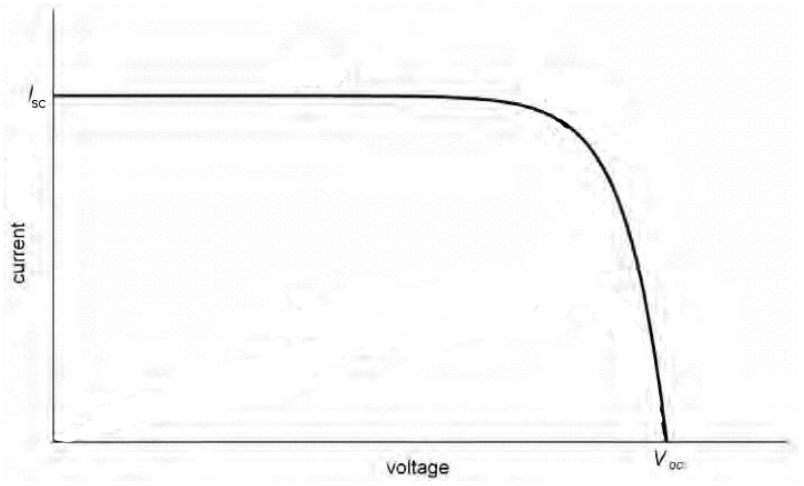

Figure 21: Typical current voltage behavior of a solar cell [7].

Equation 61 gives the type of solutions that figure 21 present. Generally, we know that electrical power is a product of current and voltage, $P = IV$. In case of a solar cell how can we know which I in range of 0 to I_{SC} and which V in range of 0 to V_{OC} to choose to calculate the power? We can find the answer for the question by investigating the inventer system under which PV-system is working.

If inventer system is so called buck converter it works at constant voltage load (see fig. 22) [6]. In this case solar sells operation voltage V can be

chosen to be same as inverters voltage load. In case of figure 22 that would be V_1. Now operating current for that certain voltage can be calculated using equation 61 and further more the operating power.

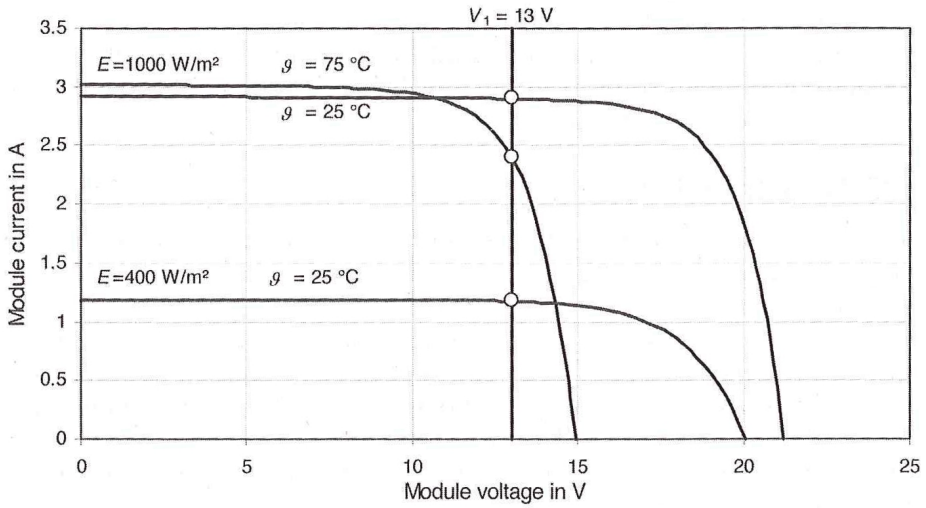

Figure 22: Illustration of buck converter's constant voltage load [6].

More common and definitely better inventer type is the so called maximum power point tracker. MPP tracker finds and operates at the voltage where product of IV generates its maximum value [6]. The point is called as maximum power point, MPP.

Solar cell V-I behavior and product of I and V are presented in figure 23. In case of figure 23 MPP tracker type of inventer would operate at voltage that is V_{MPP}. That certain operation voltage is called maximum power point voltage and we can find maximum power point current I_{MPP} by using equation 61. Product of I_{MPP} and V_{MPP} gives the maximum power point power P_{MPP} which we assume to be the solar cells operation power. We can generalize this in the following way: When assuming PV-system working under MPP tracer type of inventer we can define system power P_{MPP} using the equation 61 in a following way

$$\begin{cases} I = I_{SC}\left[1 - \exp\left(\dfrac{V + IR_S - V_{OC}}{V_t}\right)\right] \\ P = IV \\ P_{MPP} = \max\left(P\right) \end{cases} \tag{76}$$

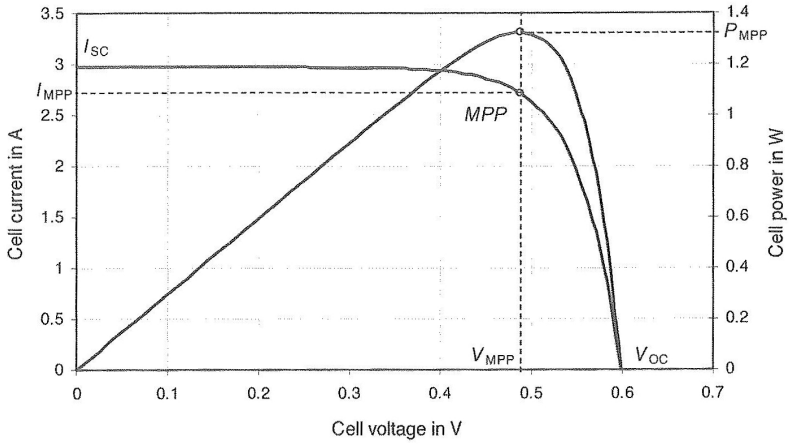

Figure 23: Solar cell's V-I and V-P behavior [6].

8 Results

8.1 Case Pitäjänmäki

In this section I have calculated the theoretical yield of solar array planned in Pitäjänmäki. At the end of this section the yield is calculated for a range of tilt and orientation angles to find out the tilt and orientation angles that lead to the greatest yield.

8.1.1 Example calculation: radiation on tilted surface

To illustrate the calculation method described in this thesis, the day of 07.08.2007 is chosen to be an example day. To receive final results, all the days from the three year data are calculated similarly like the example day. Day 07.08.2007 have been chosen randomly just to illustrate the steps of the whole calculation.

The day number for this example day is $n = 189$ and thus the declination for this day using equation 1 is $\delta = 23.448^o$. The direction of our example solar collector was chosen so that its orientation angle $\gamma = 20^o$ and its tilt angle $\beta = 30^o$. The organization which is planning to build up the solar array informed us that collectors are needed to be orientated 20^o from south to west. For this reason the orientation angle for the example calculation was chosen to be $\gamma = 20^o$. On the other hand, the sales manager of Sulwind Gylling Oy was informed by an expert that the optimum tilt angle for this array might be 30^o. For this reason the tilt angle for this example calculation was chosen to be $\beta = 30^o$.

The hours of the example day are presented in column TO in table 11 so that given hour is a starting point of the measured hour. For example hour 14 represents data which is measured from 14:00 to 15:00.

Global radiation, diffuse radiation, average ambient temperature and average wind speed for the given hour are in columns H_g, H_d, T_a and u_S, respectively. These parameters are from the data of FMI and thus radiation parameters are for horizontal surface. Beam radiations are calculated as the difference between global and diffuse radiations, $H_b = H_g - H_d$.

Hour angles are in column ω_1 and they were calculated using equation 4. Subscript 1 tells that the given hour angle is the starting point of the measured hour. Some equations require ω_2 which is the ending point of the measured hour. However, it can simply be calculated as follows: $\omega_2 = \omega_1 + 15^o$. Solving ω_2 for the last hour of the day from the equation, gives an incorrect value. However, we ignore this because the last hour of the day is at midnight and at that time no radiation occurs. Some of the equations require parameter ω and the middle points of the measured hours are chosen as values for these parameters. Thus $\omega = \omega_1 + 7.5^o$.

Extraterrestrial radiations on horizontal surface for each hour are calculated from equation 13 and are in column H_0 and the clearness indices are calculated using equation 14 and are in column k_T. Unsteady weather conditions of our example summer day can be seen in the clearness indices. The values higher than 0.8 represent clear sky, the values below 0.22 represent heavily over-casted sky and the values between these two represent the intermediate sky conditions. Extraterrestrial radiations are negative at solar night hours and they give a negative value for clearness indices at solar night hours. Negative clearness indices are not listed in table 11 and they are replaced with zeros.

If for some reason $H_{global,hor} > H_0$ then clearness index gets a value higher than one. These are unphysical situations and in these cases k_T are chosen to be one. Hour 20 in table 11 represents this kind of situation. In overall data the situation $H_{global,hor} > H_0$ happens only during sunset and sunrise hours. At these hours radiation is relatively small and thus the effect of uncertain clearness index is neglectible.

In columns $\cos\theta$ and $\cos\theta_z$ are values which are solved from equations 5 and 6, using values from tables 1 and 11 and parameters $\delta = 23.448^o$, $\beta = 30^o$ and $\gamma = 20^o$. Values in column R_b were calculated using equation 19 except for sunrise and sunset hours using equation 20.

Clearness ϵ was calculated using $\cos\theta_z$ in equation 26. Atmospheric brightness Δ was calculated using equation 29 using equations 9 and 10. Clearness and atmospheric brightness are in columns ϵ and Δ. Using clearness ϵ the correct values were found for brightness coefficients f_{11}, f_{12}, f_{13},

f_{21}, f_{22} and f_{23} from table 5. Values in columns F_1 and F_2 of table 11 were calculated using equations 27 and 28 with Δ, f_{11}, f_{12}, f_{13}, f_{21}, f_{22} and f_{23}.

Table 12 displays radiation components and total radiation on tilted surface for each hour using values from table 11 and a value of $\rho = 0.2$ as ground reflectance. Results were solved using equation 33. Ground reflectances for other days were chosen so that $\rho = 0.2$ for average thermal summer and $\rho = 0.7$ for average thermal winter according to table 1.

When we examine columns $H_{T,r}$ and H_T in table 12 we can note that $H_{T,r}$:s are about the 10^2 times smaller than H_T:s. That confirms the insignificant role of $H_{T,r}$ in H_T and at the same time it reveals that using general values from literature as ground reflectance ρ instead of estimating the precise one for the current location makes no difference in overall results.

8.1.2 Example calculation: effect of shading, glass cover and dust

The effect of shading is shown in columns $\mathrm{SE_b}$ and $\mathrm{SE_{cs}}$ of table 13. If the profile angle α_p is lower than the reference angle, that is α in the case of beam radiation and α_2 in the case of circumsolar diffuse (see fig 12), at the starting point of the measured hour ω_1 and at the end of the measured hour ω_2 then the shading effect (SE) equals zero. The shading effect equals zero also when the sun is underneath the horizon during the whole measured hour. If the profile angle is greater than reference altitude during the measured hour then the shading effect (SE) equals one.

When the profile angle has gone past the reference angle during the measured hour the shading effect has been chosen to be the relative time that the profile angle has been higher than the reference angle during the hour of issue. In case of beam radiation $\mathrm{SE_b} = (\omega_p - \omega_1)/(\omega_2 - \omega_1)$ when the sun is setting down and $\mathrm{SE_b} = (\omega_2 - \omega_p)/(\omega_2 - \omega_1)$ when the sun is rising. In case of circumsolar radiation $\mathrm{SE_{cs}} = (\omega_{p,2} - \omega_1)/(\omega_2 - \omega_1)$ when the sun is setting down and $\mathrm{SE_{cs}} = (\omega_2 - \omega_{p2})/(\omega_2 - \omega_1)$ when the sun is rising. The so called shading moment angle ω_p is the hour angle for the moment when the profile angle meets the reference angle α and ω_{p2} is the hour angle for the moment when the profile angle meets the reference angle α_2. The shading moment angles ω_p and $\omega_{p,2}$ are estimated from equation 7 iteratively using equations 1, 6 and 8.

The profile angles for measured hour can be found from equation 7 and at the starting points of measured hours they are in the column $\alpha_{p,1}$ and at the ending points of measured hours in the column $\alpha_{p,2}$ in table 13. Reference altitudes according to equations 35 and 36 are $\alpha = 13.2^o$ and $\alpha_2 = 5.56^o$ in the case of one meter high solar collector, tilted at $\beta = 30^o$ with the row distance of three meters.

Table 11: Values from the FMI database and values that were needed for calculating hourly radiation on tilted surface ($\beta = 30^o$ and $\gamma = 20^o$) and for photovalatic calculations on 7:th August 2007 (n=189). All H:s are in kJ/m^2.

TO	H_g	H_d	$T_a(^oC)$	$u_S(\frac{m}{s})$	H_b	$\omega_1(deg.)$	H_0	k_T	$\cos\theta$	$\cos\theta_z$	R_b	ϵ	Δ	$F1$	$F2$
0	0	0	15.3	3.8	0	-171.62	-523	0	-0.591	-0.111	0	-	0	0	0
1	0	0	15.3	3.6	0	-156.62	-297	0	-0.549	-0.064	0	-	0	0	0
2	14	12	15.1	3.3	2	-141.62	57	0.245	-0.455	0.011	0	4.036	0.227	0.208	0.188
3	57	54	15.3	3.3	3	-126.62	515	0.111	-0.318	0.108	0	1.121	0.106	0	-0.054
4	115	111	15.1	3.2	4	-111.62	1045	0.110	-0.145	0.219	0	1.046	0.106	0	-0.082
5	268	264	15.2	1.6	4	-96.62	1612	0.166	0.052	0.339	0.152	1.015	0.164	0.012	-0.075
6	404	399	15.4	2	5	-81.62	2176	0.186	0.258	0.458	0.563	1.012	0.183	0.032	-0.071
7	576	567	15.8	2	9	-66.62	2699	0.213	0.460	0.568	0.810	1.014	0.210	0.055	-0.066
8	969	950	17	2.5	19	-51.62	3147	0.308	0.644	0.662	0.973	1.018	0.301	0.117	-0.057
9	745	733	17	1.8	12	-36.62	3487	0.214	0.798	0.734	1.087	1.016	0.210	0.069	-0.061
10	1492	1414	18.1	1.6	78	-21.62	3697	0.404	0.911	0.778	1.171	1.053	0.382	0.174	-0.047
11	1989	1321	20	2	668	-6.62	3763	0.529	0.975	0.792	1.231	1.493	0.350	0.362	0.015
12	985	832	17.9	2.8	153	8.38	3680	0.268	0.986	0.774	1.274	1.178	0.226	0.181	-0.024
13	2271	952	18.8	1.5	1319	23.38	3453	0.658	0.944	0.727	1.299	2.313	0.275	0.491	0.100
14	2563	734	21.2	2.2	1829	38.38	3099	0.827	0.851	0.652	1.305	3.298	0.237	0.485	0.142
15	1139	650	19.6	3.8	489	53.38	2641	0.431	0.713	0.556	1.283	1.682	0.246	0.324	0.058
16	1813	797	20.1	2.5	1016	68.38	2111	0.859	0.540	0.444	1.217	2.183	0.377	0.323	0.053
17	1215	439	19.8	3.7	776	83.38	1545	0.787	0.344	0.325	1.059	2.824	0.284	0.269	0.124
18	447	234	18.3	3.6	213	98.38	980	0.456	0.138	0.206	0.669	2.216	0.239	0.286	0.117
19	86	81	16.9	3.4	5	113.38	457	0.188	-0.065	0.095	0	1.149	0.179	0.029	-0.050
20	18	17	16	2.8	1	128.38	10	1	-0.249	0.001	0	11.508	3.207	0	-3.866
21	0	0	15.5	2	0	143.38	-330	0	-0.403	-0.071	0	-	0	0	0
22	0	0	15.3	2.5	0	158.38	-541	0	-0.515	-0.115	0	-	0	0	0
23	0	0	14.8	1.9	0	173.38	-606	0	-0.580	-0.129	0	-	0	0	0

Table 12: Radiation components to tilted surface ($\beta = 30^o$ and $\gamma = 20^o$) on 7:th August 2007, using as a ground reflectance $\rho = 0.2$. All H:s are in kJ/m^2.

TO	$H_{T,b}$	$H_{T,iso}$	$H_{T,cs}$	$H_{T,hz}$	$H_{T,r}$	H_T
0	0	0	0	0	0	0
1	0	0	0	0	0	0
2	0	9	0	1	0	10
3	0	50	0	-1	1	50
4	0	104	0	-5	2	101
5	1	243	0	-10	4	238
6	3	360	7	-14	5	362
7	7	500	25	-19	8	521
8	18	783	108	-27	13	895
9	13	637	55	-22	10	692
10	91	1089	289	-34	20	1456
11	823	786	589	10	27	2235
12	195	636	192	-10	13	1026
13	1713	452	607	47	30	2851
14	2386	353	464	52	34	3290
15	627	410	271	19	15	1342
16	1236	503	313	21	24	2098
17	822	299	125	27	16	1290
18	143	156	45	14	6	363
19	0	73	0	-2	1	72
20	0	16	0	-33	0	0
21	0	0	0	0	0	0
22	0	0	0	0	0	0
23	0	0	0	0	0	0

Relative transmittances for isotropic diffuse, horizontal diffuse and ground reflectance are functions of β and dirtiness level from table 6. In this case dirtiness level is chosen to be *Medium* and tilt angle $\beta = 30^o$. Thus, relative transmittances for above mentioned radiation components are $\mathrm{FT_{iso}} = 0.9315$, $\mathrm{FT_{hz}} = 0.9154$ and $\mathrm{FT_r} = 0.7163$. Relative transmittances for beam radiation components and circumsolar radiation components are the same $\mathrm{FT_b} = \mathrm{FT_{cs}}$, which is explained in section 6. The parameters $\mathrm{FT_b}$ and $\mathrm{FT_{cs}}$ are functions of $\cos\theta$ and thus they vary at every hour. Values for $\mathrm{FT_b}$ and $\mathrm{FT_{cs}}$ are calculated using equation 49 and are in the column $\mathrm{FT_b}$&$\mathrm{FT_{cs}}$ of table 13.

When examining the table 13 it seems like SE_b and SE_{cs} have no effect because FT_b and FT_{cs} are nonzero only when SE = 1, which is true for this given day and given tilt and orientation angle. For example a higher tilt angle would give less zeros in FT column and more zeros in SE columns, and a lower tilt angle would give less zeros in SE columns and more zeros in FT column. In other words, as the chosen tilt angle is near to the optimum tilt angle(we will find out that later) FE and SE get nonzero values pretty much at the same hours.

Table 13: Values that describe effect of shading, glass cover and dust. The parameters $\alpha_{p,1}$ and $\alpha_{p,2}$ are in degrees.

TO	$\alpha_{p,1}$	$\alpha_{p,2}$	SE_b	SE_{cs}	FT_b&FT_{cs}
0	7.28	5.22	0	0	0
1	5.22	1.74	0	0	0
2	1.74	3.70	0	0	0
3	3.70	12.18	0	0.738	0
4	12.18	25.66	0.907	1	0
5	25.66	46.22	1	1	0.219
6	46.22	71.67	1	1	0.713
7	71.67	86.23	1	1	0.896
8	86.23	71.34	1	1	0.962
9	71.34	61.97	1	1	0.986
10	61.97	55.98	1	1	0.995
11	55.98	52.14	1	1	0.999
12	52.14	49.79	1	1	0.999
13	49.79	48.74	1	1	0.997
14	48.74	49.17	1	1	0.991
15	49.17	51.96	1	1	0.975
16	51.96	60.04	1	1	0.932
17	60.04	84.83	1	1	0.812
18	84.83	38.43	1	1	0.485
19	38.43	6.55	0.674	1	0
20	6.55	3.65	0	0.061	0
21	3.65	7.20	0	0	0
22	7.20	8.03	0	0	0
23	8.03	8.03	0	0	0

Table 14 shows radiation components and total radiation on tilted solar collector for each hour when taking into account shading effect, glass cover and dust. Results were solved from equations 45 and 53 using values from

previous tables in this section.

Table 14: Effective radiation components on tilted solar collector. H:s are in kJ/m^2.

TO	$H_{T,b,sh,FT}$	$H_{T,iso,sh,FT}$	$H_{T,cs,sh,FT}$	$H_{T,hz,sh,FT}$	$H_{T,r,sh,FT}$	$H_{T,sh,FT}$
0	0	0	0	0	0	0
1	0	0	0	0	0	0
2	0.0	7.8	0.0	0.0	0.0	7.8
3	0.0	44.2	0.0	0.0	0.0	44.2
4	0.0	90.9	0.0	-0.1	0.0	90.9
5	0.1	213.6	0.1	-0.2	0.0	213.7
6	1.9	316.5	4.9	-0.3	0.1	323.2
7	6.3	438.8	22.1	-0.3	0.1	467.0
8	17.2	687.4	100.6	-0.5	0.2	805.0
9	12.5	559.0	52.7	-0.4	0.1	623.9
10	88.2	956.4	278.8	-0.6	0.3	1323.0
11	797.0	690.4	570.7	0.2	0.4	2058.6
12	188.9	558.4	185.7	-0.2	0.2	933.1
13	1657.7	397.0	587.4	0.8	0.4	2643.4
14	2293.9	309.8	446.4	0.9	0.5	3051.5
15	593.3	359.8	255.8	0.3	0.2	1209.4
16	1116.8	442.1	283.0	0.4	0.3	1842.6
17	647.7	262.8	98.7	0.5	0.2	1009.9
18	67.0	137.0	21.0	0.2	0.1	225.3
19	0.0	64.4	0.0	0.0	0.0	64.4
20	0.0	13.9	0.0	-0.6	0.0	13.3
21	0	0	0	0	0	0
22	0	0	0	0	0	0
23	0	0	0	0	0	0

8.1.3 Example calculation: photovoltaic generation

To find photovoltaic yield we need to calculate the open circuit voltage and short circuit current at operating point. I_{SC} and V_{OC} can be found from equations 67 and 71 but they require parameters G_{eff}/G_{STC}, where G_{eff} is an effective irradiation on solar collector and G_{STC} an irradiation at standard test conditions, which is 1000 W/m^2. Effective irradiation on solar collector during one hour is averagely same as effective radiation on solar collector

during one hour divided by 3600s, $G_{eff} = H_{eff}/3600s$. In our case effective radiation on solar collector is $H_{T,sh,FT}$ from table 14 and thus $G_{eff}/G_{STC} = (H_{eff}/3600s)/G_{STC} = H_{T,sh,FT}/(1000\ W/m^2 * 3600\ s)$. These values are in table 15 in column G_{eff}/G_{STC}.

To calculate V_{OC} and I_{SC} we also need to know the cell temperature. Cell temperatures were calculated using two different theories. Cell temperatures from equation 72 were solved using $NOTC = 46^oC$ (table 2), $G_{eff} = H_{T,sh,FT}/3600\ s$ (table 14) and T_a (table 11) values. Cell temperatures are listed in column $T_{c,NOCT}$ in table 15. Using NOCT value straight from manufacturers data is in this case reasonable because the whole solar array is planned to be build on stands and thus air can flow freely on both sides of the solar collectors.

Cell temperatures from equation 74 are listed in column $T_{c,wind}$. Ambient temperatures T_a here are also from table 11, same as wind speeds u_S. Rest of the required values can be found from table 10 and table 15. Back surface of the Swedmodule GPV200 solar module is made of Tedlar (see table 2) [Appendix 2]. Thus we can use values for *Glass/cell/tedlar* in table 10. Averages of these cell temperatures found in two different ways are in column T_c in table 15. These values are used as cell temperature in further calculations.

Operating open circuit voltages are calculated using equation 71. Values $V_{OC,STC} = 36.6\ V$, $\alpha_V = -0.0034/K$ and $T_{STC} = 25^oC$ were taken from table 2. The parameter $\rho_{OC} = -0.04$ as it has been described in section 7.3. Results are in column V_{OC} of table 15. Equation 71 gives negative values for V_{OC} at really low radiation conditions which happens when $G_{eff}/G_{STC} \lesssim 0.007$. Those values have been chosen to be zero because it is unrealistic to assume solar array acting as a energy consumer because of low irradiation.

Operating short circuit currents calculated using equation 67 are in column I_{SC} of table 15. Equation 67 requires values for $I_{SC,STC}$, α_I and T_{STC} and the values can be found from table 2. Values for T_c can be found from table 15 and values for H_b, H_d and H_r can be found from table 14 so that $H_b = H_{T,b,sh,FT}$, $H_d = H_{T,iso,sh,FT} + H_{T,cs,sh,FT} + H_{T,hz,sh,FT}$ and $H_r = H_{T,r,sh,FT}$. Equation 67 also requires values f_b,f_d and f_r. They can be found from equation 66 using the data of table 8 since the type of solar module system in issue is polycrystalline. Equation 66 also requires values for clearness indices k_T. They can be found from table 11.

Before we can calculate the operation powers of solar module we need one more parameter and that is the series resistance of solar module. That can be found from equation 62 using values from table 2. When calculating R_S from equation 62 it has to be remembered that there is 60 solar cells in the GPV200 module. The assumption is that all solar cells in the GPV200 module are in series and thus we use as a diode factor $m = 60 \cdot$ (diode factor). We do not

have the information about diode factor of solar cell in the GPV200 module. On the other hand, reference [4] claims that it is reasonable to use diode factor = ideal diode factor = 1 in this kind of calculations. Thus $m = 60$ and using this we receive the result $R_S = 0.515\ \Omega$ [4].

Maximum operating powers of solar module were solved from equation 76 iteratively and they are listed in table 15 in column P_{MPP}. If we compare this column to column H_g from table 11 we note that only radiation in scale of 100 kJ/m^2 in hour can cause reasonable power output from PV-system. Maximum *Watt-peak* power which is same as the operating power at standard test conditions can be found from manufacturers data [Appendix 2] and it is 203.3 W. All operating powers in column P_{MPP} are much smaller than watt peak power which describes the feebleness of real operating conditions compared to standard test condition.

As it was planned to have the total of 700 modules in the whole solar power plant system, the total energy output for each hour is $E_{hour} = 700 \cdot P_{MPP} \cdot 3600\ s$. Those values are listed in the column E_{hour} of table 15.

Now we can calculate the total energy production for whole day (07.08.2007) and that is $E_{day} = \sum_{TO=0}^{23} E_{hour} = 2.276\ GJ$.

8.1.4 Final result: tilt and orientation angle effect on yield

There was the total of 1096 days in the data from Finnish Meteorological Institute (years 2007-2009). Matlab software [15] was used to calculate E_{day} for all of the days, in the same way as it has been described previously in this section. The total energy production for all the three year is $E_{2007-2009} = \sum_{day=1}^{1096} E_{day} = 1.489\,TJ$. This result was received using the tilt angle $\beta = 30^o$ and the orientation angle $\gamma = 20^o$. Thus we define labeling $E_{2007-2009}(\beta = 30^o, \gamma = 20^o) = 1.489\ TJ$.

When doing these calculation all over again with different tilt angles, in range of $\beta = [0, 90^o]$ and with different orientations, in range of $\gamma = [-90^o, 90^o]$ we receive $E_{2007-2009}(\beta, \gamma)$. The result can be described best with following 3D graph in figure 24.

Top of the mountain is 1.507 TJ high and its coordinates are $\beta = 28.6^o$ and $\gamma = 0.1^o$.

The starting point requirement for orientation was that the rows needed to be orientated in a direction of $\gamma = 20^o$. Cross-section from figure 24 at point $\gamma = 20^o$ is illustrated in figure 25. The top of cross-section is at the height of 1.489 TJ and it can be received with tilt angle $\beta = 28.5^o$.

Table 15: Parameters to calculate total energy output of PV array and total energy output of PV array for each hour. $T_{c,NOCT}$, $T_{c,wind}$ and T_c are in ^oC. V_{OC} is in V, I_{SC} is in A, P_{MPP} is in W and E_{hour} is in MJ.

TO	G_{eff}/G_{STC}	$T_{c,NOCT}$	$T_{c,wind}$	T_c	V_{OC}	I_{SC}	P_{MPP}	E_{hour}
0	0	15.3	15.3	15.3	0	0	0	0
1	0	15.3	15.3	15.3	0	0	0	0
2	0.002	15.2	15.2	15.2	0	0.00	0	0
3	0.012	15.7	15.6	15.6	8.5	0.11	0.5	1.3
4	0.025	15.9	15.7	15.8	17.3	0.24	2.9	7.3
5	0.059	17.1	16.9	17.0	25.6	0.55	10.9	27.5
6	0.090	18.3	17.8	18.1	28.8	0.83	18.8	47.4
7	0.130	20.0	19.3	19.7	31.0	1.18	29.1	73.3
8	0.224	24.3	22.8	23.5	33.5	1.88	49.9	125.6
9	0.173	22.6	21.8	22.2	32.4	1.59	40.8	102.9
10	0.368	30.0	28.5	29.3	34.6	2.85	77.4	195.0
11	0.572	38.6	35.5	37.1	34.7	4.21	111.2	280.2
12	0.259	26.3	24.4	25.4	33.9	2.27	60.7	152.8
13	0.734	42.7	39.8	41.2	34.4	5.26	135.2	340.8
14	0.848	48.7	43.7	46.2	33.9	5.82	144.8	365.0
15	0.336	30.5	27.3	28.9	34.4	2.65	71.6	180.4
16	0.512	36.7	33.3	35.0	34.7	3.28	88.4	222.8
17	0.281	28.9	26.3	27.6	33.9	1.88	50.7	127.7
18	0.063	20.3	19.8	20.0	25.8	0.46	9.1	23.0
19	0.018	17.5	17.3	17.4	13.2	0.14	1.2	3.1
20	0.004	16.1	16.1	16.1	0	8.34	0	0
21	0	15.5	15.5	15.5	0	0	0	0
22	0	15.3	15.3	15.3	0	0	0	0
23	0	14.8	14.8	14.8	0	0	0	0

8.2 Case Viitasaari

Similar calculations were done for the Viitasaari solar array. The exceptions in the calculation methods compared to previous section are brought out in this section. The day of 01.09.2008 (n=254) was chosen as a day to demonstrate calculation methods. The results in sector of radiation are in table 16. Data in columns TO and $H_g(L)$ was taken straight from University of Jyväskylä database. The values for radiation in column $H_g(L)$ are in units of *Langley*. They are converted to kJ/m^2 by factor 41.840 $kJ/Langley \cdot m^2$. The results are in column H_g of table 16.

The hour angles were calculated using equation 4 and the summer time

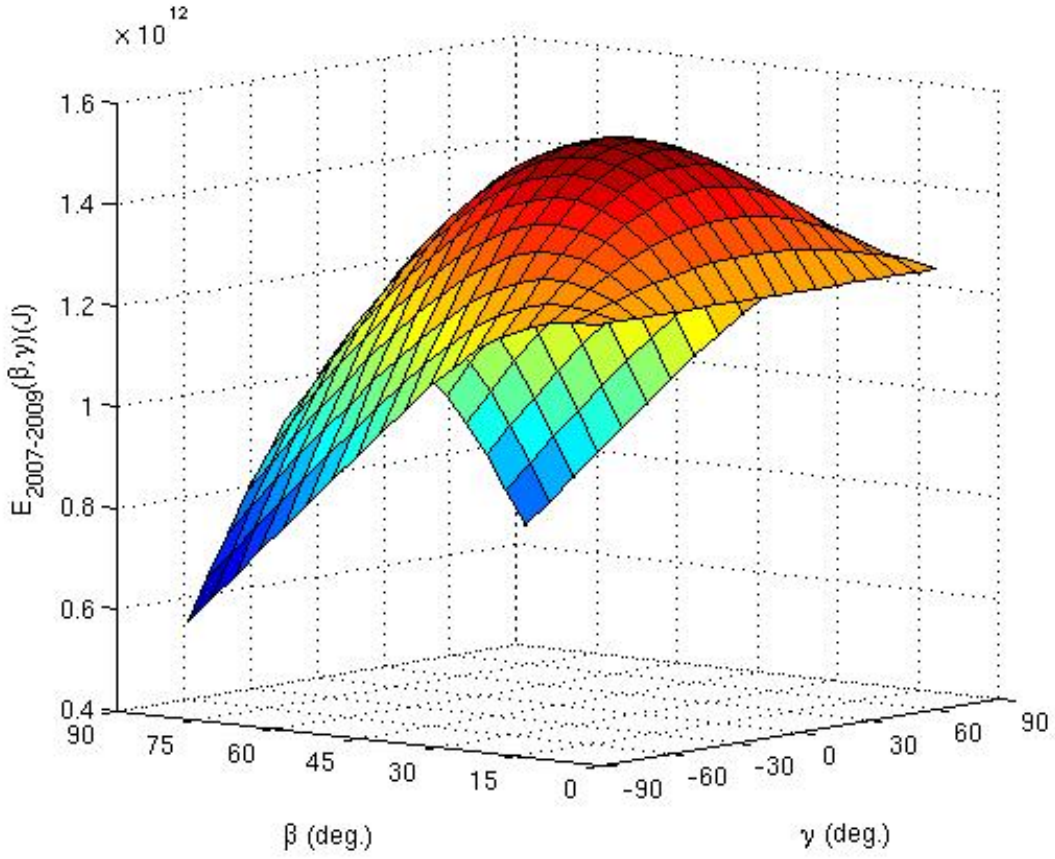

Figure 24: Function of $E_{2007-2009}(\beta, \gamma)$ for Pitäjänmäki.

was taken into account so that $AO = 1$ and the winter time so that $AO = 0$. The hour angles are in column ω_1 representing the starting point of the measured hour.

The main difference between calculations for Pitäjänmäki and Viitasaari is that there is no diffuse radiation data available from Viitasaari. Thus, we do not know the difference between diffuse and beam radiation on horizontal surface. With our initial values we can calculate extraterrestrial radiation on horizontal surface using equation 13 and with that information clearness index using equation 14. Those parameters are in columns H_0 and k_T respectively.

Negative H_0 values represent extraterrestrial radiation when sun's position is underneath horizon. Those values give negative clearness indices. In the sense of clearness index definition these values are not realistic. Thus, all clearness indices are limited so that $0 \leqslant k_T \leqslant 1$. In overall data these

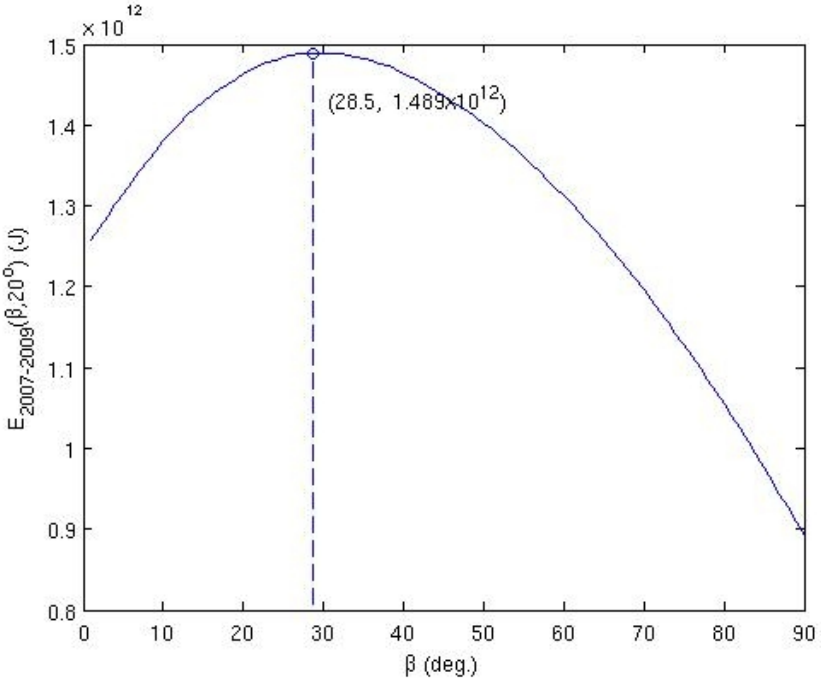

Figure 25: Function of $E_{2007-2009}(\beta, \gamma = 20^o)$ for Pitäjänmäki.

exceptions occur sometimes in the first and last measured hour of the day. In those cases the sun was theoretically beneath the horizon but measurement system was still receiving some radiation. In this kind of situation choosing k_T to be zero is reasonable since $k_t = 0$ means that all measured global radiation is considered to be as diffuse radiation in calculations (see fig 6).

By using clearness index k_T we estimated diffuse radiation on horizontal surface using equation 15. Results are in column H_d of table 16. Beam radiations on horizontal surface are $H_b = H_g - H_d$ and they are in column H_b.

Figure 26 is here to demonstrate the way equation 15 works. All four curvatures were drawn using data from table 16. Clearly the morning was clear and the noon was cloudy during the example day. In the morning global radiation is near to extraterrestrial radiation and at noon it is much below the extraterrestrial radiation. Because in the morning there is a lot of global radiation equation 15 expects there to be a lot of beam radiation. At noon there is little global radiation compared to extraterrestrial radiation so equation 15 expects it all to be almost entirely diffuse radiation.

Because solar array in Viitasaari is tilted at $\beta = 5^o$ and orientated at $\gamma = 0$ we use these values to calculate radiation components on tilted surface

Table 16: Horizontal radiation components from Viitasaari at 10.09.2008. H:s are in kJ/m^2 except $H_g(L)$ which is in Langley.

TO	ω_1	$H_g(L)$	H_g	H_0	k_T	H_d	H_b
0	-198.35	0	0	-1865	0	0	0
1	-183.35	0	0	-1898	0	0	0
2	-168.35	0	0	-1783	0	0	0
3	-153.35	0	0	-1526	0	0	0
4	-138.35	0	0	-1146	0	0	0
5	-123.35	0	0	-667	0	0	0
6	-108.35	0.93	39	-124	0	39	0
7	-93.35	6.36	266	448	0.595	120	146
8	-78.35	14.56	609	1008	0.604	262	347
9	-63.35	23.30	975	1520	0.641	342	633
10	-48.35	29.95	1253	1948	0.643	435	818
11	-33.35	39.33	1646	2263	0.727	339	1306
12	-18.35	50.39	2108	2443	0.863	348	1760
13	-3.35	23.90	1000	2476	0.404	834	166
14	11.65	15.26	638	2361	0.270	616	22
15	26.65	13.19	552	2104	0.262	535	17
16	41.65	14.26	597	1724	0.346	542	55
17	56.65	12.29	514	1245	0.413	422	92
18	71.65	8.63	361	702	0.514	227	134
19	86.65	2.30	96	130	0.738	19	78
20	101.65	0.07	3	-430	0	3	0
21	116.65	0	0	-942	0	0	0
22	131.65	0	0	-1370	0	0	0
23	146.65	0	0	-1685	0	0	0

on our example day. Results can be seen from table 17. The value of $\rho = 0.2$ was used as ground reflectance. In overall data a ground reflectance $\rho = 0.2$ was used when the day was at thermal summer and $\rho = 0.7$ when the day was at thermal winter according to table 3.

To calculate relative transmittances *dirtiness* level *high* from table 6 were used. It has been chosen *high* because no proper service was established to Viitasaari solar array. Relative transmittances for the beam and the circumsolar radiation components are in column $\mathrm{FT_b}$ of table 17. For chosen tilt angle relative transmittances for isotropic diffuse, horizontal diffuse and ground reflectance are $\mathrm{FT_{iso}} = 0.896$, $\mathrm{FT_{hz}} = 0.283$ and $\mathrm{FT_r} = 0.166$ respectively.

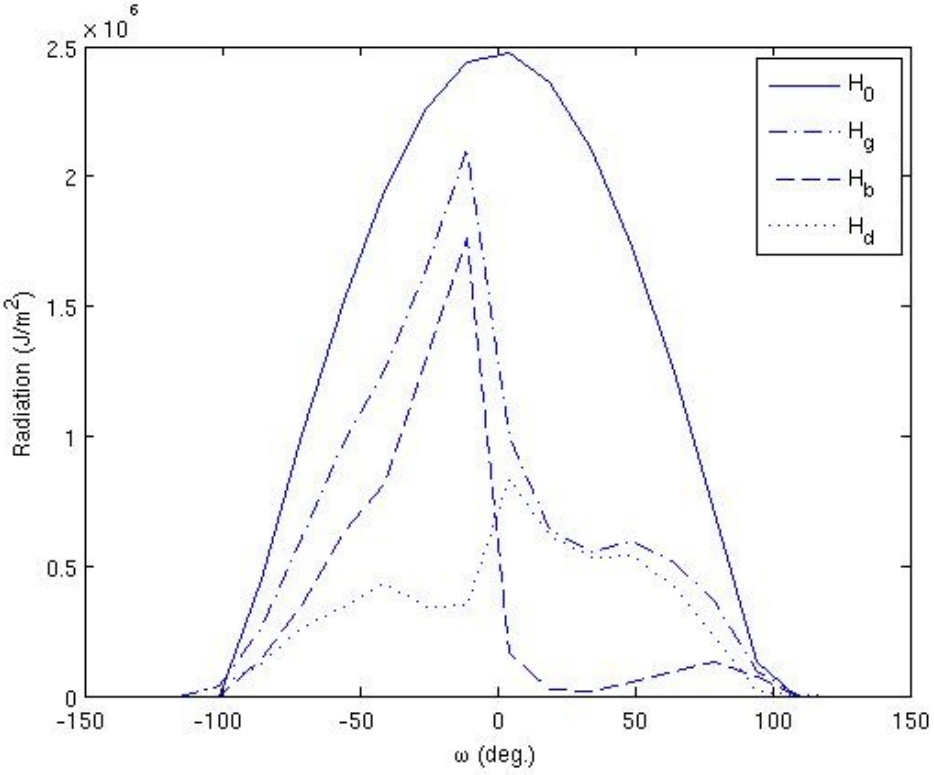

Figure 26: Extraterrestrial, global, beam and diffuse radiation on day 10.09.2008 from Viitasaari

In Viitasaari case no shading effect occurs. The whole solar array is on a flat plane which eliminates the self shading. There is a lake in the front of the solar array which causes no shading effect either. Effective radiation on solar array was calculated by taking only into account the effect of the glass cover and the dust. The results are in column $H_{T,FT}$ of table 18.

In columns T_a and u_S of table 18 are the average ambient temperatures and wind speeds from the data base of the University of Jyväskylä. Those values and the values from tables 4, 9 and 17 were used to calculate the operating open circuit voltage and short circuit current, which can be found in columns V_{OC} and I_{SC}. NOCT value to calculate cell temperature was not found in the manufacturer's data sheet. Thus, we use the average one which is 44^oC especially because air can flow on the both sides of solar modules. Maximum power point powers are in column P_{MPP}. There is a total 154 modules installed in solar array. The number of modules was used to calculate energy produced by whole solar array during the measured hours. Results are in column E_{hour}.

Table 17: Radiation components on tilted surface ($\beta = 5^o$ and $\gamma = 0$) and relative transmittance for beam and circumsolar diffuse radiation components for Viitasaari at 10.09.2008. H:s are in kJ/m^2

TO	$H_{T,b}$	$H_{T,iso}$	$H_{T,cs}$	$H_{T,hz}$	$H_{T,r}$	H_T	$\mathrm{FT_b}$
0	0	0	0	0	0	0	0
1	0	0	0	0	0	0	0
2	0	0	0	0	0	0	0
3	0	0	0	0	0	0	0
4	0	0	0	0	0	0	0
5	0	0	0	0	0	0	0
6	0.0	38.8	0.0	-0.4	0.0	38.5	0.000
7	150.2	97.0	23.6	1.6	0.1	272.4	0.303
8	383.9	188.8	80.7	2.5	0.2	656.1	0.587
9	712.9	226.1	130.4	5.2	0.4	1074.9	0.748
10	929.4	274.9	181.0	4.7	0.5	1390.6	0.836
11	1489.3	192.9	166.7	7.0	0.6	1856.6	0.882
12	2011.0	188.2	182.0	7.3	0.8	2389.2	0.903
13	189.3	663.5	193.7	-2.0	0.4	1045.0	0.907
14	25.1	566.5	55.8	-3.5	0.2	644.2	0.894
15	19.4	495.6	43.5	-3.1	0.2	555.7	0.860
16	61.9	453.4	99.3	-1.6	0.2	613.2	0.794
17	103.3	329.3	102.7	0.0	0.2	535.5	0.671
18	144.7	174.4	56.4	1.5	0.1	377.2	0.450
19	67.4	14.1	1.0	0.6	0.0	83.0	0.067
20	0.0	2.9	0.0	0.0	0.0	2.9	0.000
21	0	0	0	0	0	0	0
22	0	0	0	0	0	0	0
23	0	0	0	0	0	0	0

Sum of the energies of all hours during the years 2006-2008 is $E_{2006-2008}(\beta = 5, \gamma = 0) = 38.08\ GJ$.

By doing the calculations with different tilt angles in range of $\beta = [0, 90]$ and with different orientation angles in range of $\gamma = [-90, 90]$ we receive $E_{2006-2008}(\beta, \gamma)$ and the result can be seen in figure 27. The highest energy can be received with tilt angle $\beta = 46.4^o$ and orientation angle $\gamma = -4.3^o$ and that is $E_{2006-2008}(\beta = 46.4, \gamma = -4.3) = 47.76\ GJ$.

Table 18: Effective radiation on tilted surface and photovoltaic generation from Viitasaari at 10.09.2008 when $\beta = 5^o$ and $\gamma = 0$. $H_{T,FT}$ is in kJ/m^2, T_a is in ^oC, u_S is in m/s, V_{OC} is in V, I_{SC} is in A, P_{MPP} is in W and E_{hour} is in kJ.

TO	$H_{T,FT}$	T_a	u_S	V_{OC}	I_{SC}	P_{MPP}	E_{hour}
0	0	8.12	4.29	0	0	0	0
1	0	7.72	4.37	0	0	0	0
2	0	7.16	4.07	0	0	0	0
3	0	7.07	4.16	0	0	0	0
4	0	6.82	4.07	0	0	0	0
5	0	6.59	3.82	0	0	0	0
6	32	6.32	4.09	5.5	0.03	0.1	30
7	129	6.23	4.85	28.9	0.03	0.7	401
8	407	6.66	4.93	41.7	0.11	3.7	2068
9	768	7.61	4.64	46.0	0.21	7.7	4286
10	1082	8.76	3.88	47.3	0.30	11.0	6085
11	1505	9.68	5.47	48.2	0.42	14.9	8271
12	1980	10.40	5.77	48.3	0.54	18.3	10144
13	866	10.26	5.31	46.2	0.26	9.3	5160
14	533	10.37	4.62	43.3	0.17	5.9	3294
15	458	10.32	4.49	42.2	0.15	5.0	2770
16	491	10.38	3.90	42.7	0.15	5.1	2823
17	399	10.41	4.54	41.0	0.12	3.8	2094
18	227	9.84	5.09	35.6	0.06	1.7	952
19	16	9.08	5.25	0.0	0.00	0.0	0
20	2	7.94	4.69	0.0	0.00	0.0	0
21	0	7.47	3.71	0	0	0	0
22	0	7.52	3.46	0	0	0	0
23	0	7.35	3.30	0	0	0	0

9 Discussion

Energy produced The whole solar array at Viitasaari produced 18.18 GJ of energy during the years 2006-2008. That was measured by the inventer system. The measured value is dramatically lower than our estimated value $E_{2006-2008}(\beta = 5, \gamma = 0) = 38.08\ GJ$. According to Ref. [13] one of the reasons for causing this difference is the oversized inverter system. Besides, the inventer efficiency was not calculated in this thesis. However, we believe that the biggest reason for the poor energy production might be that the solar array had not been serviced at all. Six modules have cracked during its

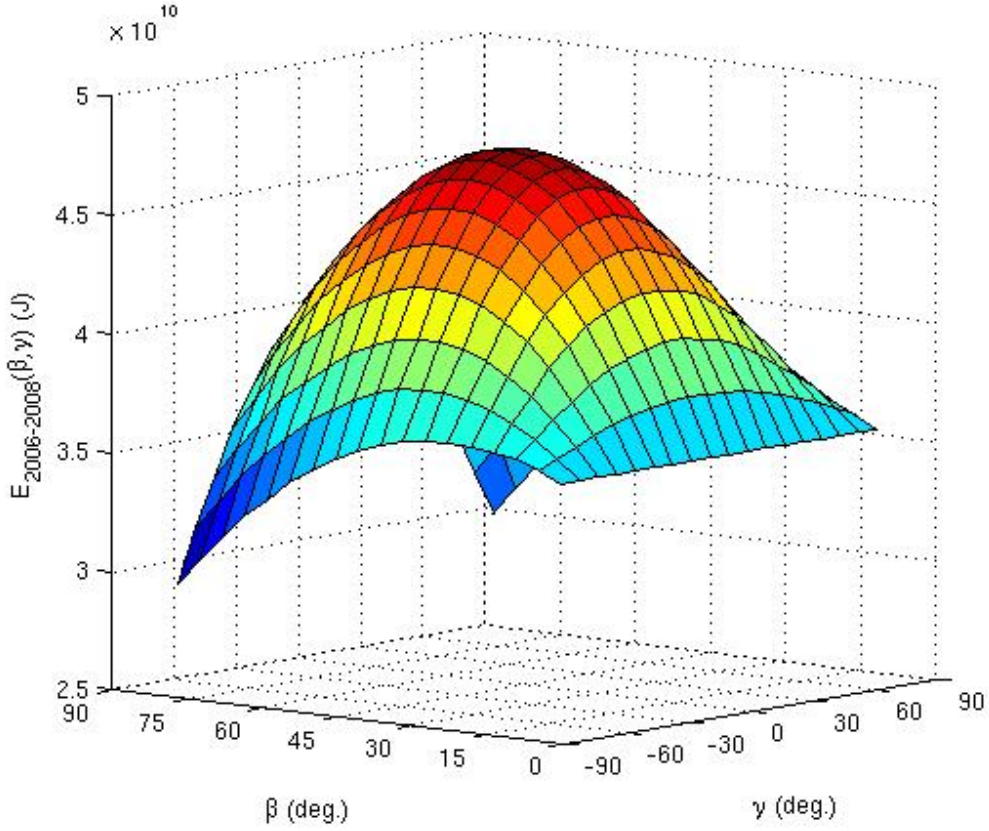

Figure 27: Function of $E_{2006-2008}(\beta, \gamma)$ for Viitasaari

operation time. One cracked module in the series of modules will destroy the whole series power output. Delayed correction has probably been reducing the total energy produced. Also cracked modules have not been replaced but they have been connected out from series. That naturally reduces the number of modules in whole solar array.

Still, the biggest service issue might be the snow. Typically snow melts and glides away off the solar module when solar radiation warms up the dark surface of solar module. This solar array is transparent and lowly tilted, and both of these characteristics lower the melting and gliding effect. In addition there has been no effort to remove the snow from solar array.

Nowadays Pitäjänmäki solar power plant is functional. Actual size of solar power plant is slightly bigger than the one estimated in this work. Reference [17] reported that in Pitäjänmäki power plant there are 870 collector in array so that rated power is 181 kWp. Approximate energy production per year

was reported to be 160 000kWh which is 1.728 TJ for three years. Power plant size in this thesis was estimated to be 700 collectors with rated power of 140 kWp. Our estimation for the three years energy production with optimal tilt angle was 1.489 TJ.

Tilt and orientation angle Typically optimum tilt angle was informed to be $Latitude \pm 10^o$ or from $Latitude$ to $Latitude - 10^o$ in many references for example like in ref. [3] and [5]. According to this information the optimum tilt angle for Pitäjänmäki would be 60^o or 50^o and for Viitasaari 63^o or 53^o. Both are higher that the estimated ones in this work.

The most sophisticated way to estimate optimum tilt angle for fitted solar collector was found from [4]. They present function

$$\beta_{opt} = 3.7 + 0.69\phi \tag{77}$$

This function has been received by estimating optimum tilt angles for solar collectors for various geographical locations and creating curve-fitting as a function of ϕ. The function will give optimum tilt angle for Pitäjänmäki as $\beta_{opt} = 3.7 + 0.69 * 60.12^o \approx 45^o$ and for Viitasaari as $\beta_{opt} = 3.7 + 0.69 * 63.07^o \approx 47^o$. In this work the estimated optimum tilt angle for Pitäjänmäki is $\beta_{opt} = 28.6^o$ and for Viitasaari is $\beta_{opt} = 46.4^o$.

In case Pitäjänmäki there was shading occurring and in case Viitasaari there was not. Thus it seems like equation 77 gives a good approximation about optimum tilt angle when shading effect is not involved. When shading effect is involved then equation 77 is more or less useless.

Accuracy of equation 77 is only two digits. For this reason it might be a good tool for estimating optimum tilt angle for household scale installations. For power plant scale installations, which was the case in Pitäjänmäki, more precise and detailed estimations like one presented in this work are required.

In both cases of Pitäjänmäki and Viitasaari maximum energy producing tilt angles $\beta_{opt} = 28.6^o$ and $\beta_{opt} = 46.4^o$ are lower than local latitudes $\phi = 60.12^o$ and $\phi = 63.07^o$. This is because more isotropic diffuse irradiation can be received on surface with lower tilt angle. On the other hand, lowering the tilt angle from latitude angle reduces beam irradiation, circumsolar diffuse irradiation, horizontal diffuse irradiation and ground reflected irradiation on surface. Because of that $0 < \beta_{opt} < \phi$.

Maximum energy producing tilt angle for Pitäjänmäki is much smaller than maximum energy producing tilt angle for Viitasaari even when there is no significant difference between latitudes. This is due to the shading effect which occurs at Pitäjänmäki. The higher the tilt angle of the rows of solar modules the higher the effect of shading they cause on each other. This can

be also noted when comparing shapes of the curvatures from figures 24 and 27. In case of figure 24 a strong reduction of total energy output can be noted when $\beta > 28.6^o$. Actually, in the case of row installation, it seems that rows that are not tilted give reasonable energy output. That is $E(\beta = 0, \gamma)$ in figure 24. Still it is not reasonable to leave solar collectors without tilting because tilting the solar collector to the right tilt angle gives higher energy output and reduces problems with dirt and snow.

The orientation that gives the maximum energy is towards the south in Pitäjänmäki case and slightly from south to east in Viitasaari case. East is the direction where the sun rises up. Thus, the negative γ favors the morning radiation more than the noon radiation. The reason for that can be understood easily when we examine the measured global radiation data from Viitasaari. The total global radiation during the years 2006-2008 at Viitasaari was 8.338 GJ/m^2. Total 4.248 GJ/m^2 of that was radiated at solar morning ($\omega < 0$) and 4.091 GJ/m^2 was radiated at solar noon ($\omega > 0$).

Effect of over-tilting Effect of over tilting is illustrated in figure 28. Over-tilting the solar collector can get slightly higher radiation yields for winter months. The price for over-tilting is the strong reduction of total radiation yield due to the reduction of yields of high irradiation summer months. Thus, it is a decision of solar array builders whether they try to make annual energy yield distribution smoother at the expense of total yield reduction. Doing smoother annual energy yield distribution could be reasonable in the case of solar heat collectors but probably not in the case of grid connected PV-systems.

How different components of this work have effect on optimum tilt angle In Pitäjänmäki case if we investigate what would be the optimum tilt angle taking account only the radiation on tilted surface then $\beta_{opt} = 43.3^o$. This result has been received using theories from section 4 and finding out the tilt angle that causes the highest radiation on tilted surface. When shading theories from section 5 are added to previous we receive $\beta_{opt} = 28.1^o$. With this tilt angle the highest radiation will be received on surface when it is shaded in such a way that is described in section 1. If the effect of glass cover and dust theories from section 6 are added with all the previous then $\beta_{opt} = 30.9^o$. And finally when Photovoltaic generation from section 7 is taken account we receive the final result about optimum tilt angle and that is $\beta_{opt} = 28.6^o$.

So what is happening? Using only radiation the result is $\beta_{opt} = 43.3^o$. This is pretty reasonable in many ways. All the narrow theories like equation

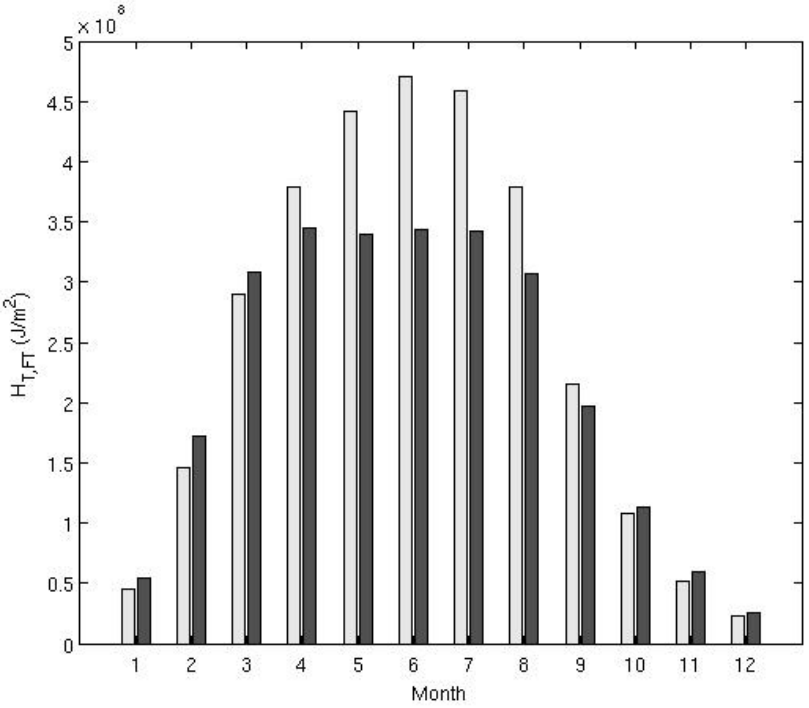

Figure 28: Effect of over-tilting. Left/lighter bars describe average monthly effective radiation distribution in case of Viitasaari when $\beta = \beta_{opt} = 46.4^o$ and $\gamma = \gamma_{opt} = -4.3^o$, right/darker bars describe average monthly effective radiation distribution in case of Viitasaari when $\beta = 80.0^o$ and $\gamma = \gamma_{opt} = -4.3^o$

77 are predicting something like this.

When shading effect is included the result changes dramatically to $\beta_{opt} = 28.1^o$. The result is much lower optimum tilt angle. Reason for this is that higher tilt angle in rows causes higher shading effect. Because of this the shading effect theory favors lower tilt angles like $\beta_{opt} = 28.1^o$.

When the effect of glass cover and dust has been taken account then the result rises again ($\beta_{opt} = 30.9^o$). Glass is the most transparent for illumination when the illumination meets the glass with low inclination angle. Averagely inclination angles are lowest when solar collector is tilted to latitude. In Pitäjänmäki case that is 60.12^o. For this reason the Effect of glass cover and dust theory change the optimum tilt angle a slightly towards to latitude value.

When photovoltaic generation has been taken into account then optimum tilt angle value drops again ($\beta_{opt} = 28.6^o$). This can be explained with the fact

that how solar cell responds on different irradiation levels. Solar cell operates poorly when irradiation level is below $200W/m^2$. During the morning and late noon this sort of irradiation level is more common than in middle of the day. On the other hand collectors that are tilted with high tilt angle receive better morning and late noon irradiation and collectors which are tilted with low tilt angle receive better high level middle day irradiation.

10 Conclusions

Radiation mostly defines the final yield of solar array. If there is no radiation there is no yield and if there is a lot of radiation then a big yield is available. Thus, we expect that calculations about radiation on tilted surface plays the biggest role in our estimation. This is why the most accurate calculation method available today to calculate radiation on tilted surface was chosen to be used here. The method used here is the Perez model that splits radiation in five components and is based on anisotropic sky assumption.

In tentative calculations that were done for Sunwind Gylling Oy before this thesis work, the biggest yearly radiation on tilted surface producing tilt angle β was calculated using *isotropic sky* assumption, equation 25 and data of year 2009 from Helsinki Kumpula. The shading effect was assumed to be shading effect for solar collector (not PV-system). The highest energy producing tilt angle was $\beta_{opt} = 15.0^o$ when orientation was chosen to be $\gamma = 20$.

Isotropic sky assumption overestimates the isotropic diffuse radiation component because it assumes all diffuse radiation to be isotropic. Isotropic diffuse radiates equally from all over the skydome, and therefore it favors the surfaces with low tilt angles like $\beta_{opt} = 15.0^o$. Perez model reduces the weight of isotropic diffuse and spreads it more reasonably between three different diffuse radiation components. The result is higher maximum energy yield producing tilt angle like $\beta_{opt} = 28.6^o$.

Shading effect needs to be taken into consideration if it occurs. Proof for that is two dramatically deviating optimum tilt angles from Helsinki Pitäjänmäki ($\beta_{opt} = 28.6^o$) and from Viitasaari ($\beta_{opt} = 46.4^o$). Effect of shading limits the directions where radiation is coming from, thus the estimations were done taking account only the available radiation at shaded circumstances.

Almost all solar collectors are covered by glass or by materials that behave like glass under illumination. Taking into account every collector's glass cover characteristics is complex. We believe that the method used here which reduces radiation with high inclination angles is proper in all cases. It describes well the typical characteristics of angle dependent transparency of glass that is covered by dust. The effect of the method to the final result is that it favors the tilt and orientation angles which give the low inclination angles to the high radiation hours.

In case of PV-systems the electrical behavior of solar cell is taken into

account. That is because PV-system is not functional at extremely low irradiation conditions, and on the other hand it gives some estimation about yield of planned solar array. One ideal diode model, was used in our calculations because we wanted to do calculations using the data only described typically in manufacturers data. One ideal diode model overestimates the power produced by solar cell [4]. That should be taken into account when considering our results about final yields for solar arrays. Calculating maximum energy producing tilt and orientation angle, the energy production level has no effect because its a relative (less solar modules in a system causes less produced energy, but it has no effect on β_{opt} and γ_{opt}). The electrical characteristics of solar cell have effect on β_{opt} and γ_{opt} because it stresses radiation hours and radiation components that lead to the greatest energy production and does not stress low irradiation level conditions when PV-system is hardly functional at all. One ideal diode model takes into account the typical electrical characteristics of solar cell, especially when we consider the behavior of short circuit current and open circuit voltage under real operation conditions.

The measurement data for the three years was used in both cases of Pitäjänmäki and Viitasaari. To calculate the maximum energy producing tilt and orientation angles, the three year measurement data produces a reasonable approximation about radiation and weather conditions compared to average. Although, its an undeniable fact that more years would give better approximation. Those three years were sectioned in hours and all hours were separately examined as follows: how much radiation would occur on a tilted surface, how much radiation would be lost caused by shading, how much radiation would go through dirt cover and glass, and finally how much energy would the PV-system produce from that radiation in existing weather conditions. Thus, we believe that our method is adequately accurate to calculate an β_{opt} and γ_{opt} for any solar array.

References

[1] J. A. Duffie, W. A. Beckham, *Solar energy thermal processes*, New York: John Wiley & Sons Inc, 1974.

[2] A. B. Meinel, M. P. Meinel, *Applied solar energy, an introduction*, Addison-Wesley Publishing Company inc, 1976.

[3] J. A Duffie, W. A. Beckham, *Solar engineering of thermal processes*, 2nd ed., New York: John Wiley & Sons Inc, 1991.

[4] A. Luque, S. Hegedus, *Handbook of photovoltaic science and engineering*, N.J.: John Wiley & Sons Ltd, 2003.

[5] A. Goetzberger, V. U. Hoffmann, *Photovoltaic Solar Energy Generation*, Berlin: Springer-Verlag, 2005.

[6] V. Quaschning, *Understanding renewable energy systems*, London: Carl Hanser Verlag GmbG & Co KG, 2005.

[7] S. R. Wenham et al., *Applied Photovoltaics*, London: Earthscan Publications, 2006.

[8] R. Perez et al., "Modeling daylight availability and irradiance components from direct and global irradiance," *Solar Energy*, Vol. 44, No. 5, pp. 271-289, 1990. [Online]. Available: ScienceDirect, `http:\\www.sciencedirect.com`. [Accessed: March 13, 2010].

[9] L. Stamenic, E. Smiley, K. Karim, "Low light conditions modeling for building integrated photovoltaic (BIPV) systems," *Solar Energy*, Vol. 77, pp. 37–45, April 2004. [Online]. Available: ScienceDirect, `http:\\www.sciencedirect.com`. [Accessed: March 19, 2010].

[10] D. G. Erbs, S. A. Klein, J. A. Duffie, "Estimation of the diffuse radiation fraction for hourly, daily and monthly-average global radiation," *Solar Energy*, Vol. 28, No. 4, pp. 293-302, 1982. [Online]. Available: Google Scholar, `http://scholar.google.fi`. [Accessed: March 15, 2011].

[11] N. Martin, J. M. Ruzi, "Calculation of the PV modules angular losses under field conditions by means of an analytical model," *Solar Energy Materials & Solar Cells*, Vol. 70, pp. 25-38, December 2001. [Online]. Available: ScienceDirect, `http:\\www.sciencedirect.com`. [Accessed: March 15, 2011].

[12] N. Martin, J. M. Ruiz, "A New Method for the Spectral Characterisation of PV Modules," *Progress in Photovoltaics: Research and Applications* Vol. 7, No 4, pp. 299-310, January 1999. [Online]. Available: Wiley Online Library, `http://onlinelibrary.wiley.com`. [Accessed: Dec 20, 2011].

[13] D. Yang, "Performance Analysis of a Grid Connected Hybrid Photovolatic and Wind Electricity Generation System in Cold Climate," Master's Thesis, University of Jyväskylä, Jyväskylä, 2007.

[14] "Talvisään tilastoja," *Finnish Meteorological Institute*. [Online]. Available: http://ilmatieteenlaitos.fi/talvitilastot. [Accessed: April 8, 2010].

[15] "MATLAB - The Language Of Technical Computing," *MathWorks*. [Online]. Available: http://www.mathworks.com/products/matlab. [Accessed: April 17, 2010].

[16] "Southwest energy efficiency project," *SWEEP*. [Online]. Available: http://www.swenergy.org/publications/casestudies/arizona/tucson_sesc.htm. [Accessed: Muy 7, 2010].

[17] "ABB tekee aurinkosähköä taajuusmuuttajatehtaan käyttöön," *Teknologia Teollisuus*, Aug. 25, 2010, [Online]. Available: http://www.teknologiateollisuus.fi. [Accessed: Dec. 20, 2011].

[18] E. Smiley, L. Stamenic, J. Jones, M. Stojanovic, *Sixteenth European Photovoltaic Solar Energy Conference*, pp. 2002-2004, 2000.

[19] L. King, J. Kratochvil, E. Boyson, W. Bower, *2nd World Conference on Photovoltaic Solar Energy Conversion*, pp. 1947-1952, 1998.

Nomenclature

Symbol	Name
AM	Air mass [unitless]
H_b	Beam radiation $[J/m^2]$
H_d	Diffuse radiation $[J/m^2]$
H_g	Global radiation $[J/m^2]$
H_T	Radiation on tilted surface $[J/m^2]$
I_{SC}	Short circuit current [A]
I_{MPP}	Maximum power point current [A]
LH	Longitude of local timezone [deg.]
LL	Local longitude [deg.]
$NOCT$	Normal operating cell temperature [Celsius deg.]
V_{OC}	Open circuit voltage [V]
V_{MPP}	Maximum power point voltage [V]
m	Diode factor [unitless]
n	Number of day of the year [unitless]
Δ	Atmospheric brightness [unitless]
α_I	Temperature coefficient for current [1/K]
α_p	Profile angle [deg.]
α_s	Solar altitude angle [deg.]
α_V	Temperature coefficient for voltage [1/K]
β	Tilt angle of solar collector [deg.]
γ	Surface orientation angle [deg.]
γ_s	Solar azimuth angle [deg.]
δ	Declination [deg.]
ϵ	Clearness [unitless]
θ	The angle of incidence on tilted surface [deg.]
θ_z	Zenith angle [deg.]
ρ	Ground reflectance [unitless]
ϕ	Local latitude [deg.]
ω	Hour angle [deg.]
ω_1	Starting time of measured hour [deg.]
ω_2	Ending time of measured hour [deg.]

SWEDMODULE GPV200-GPV230

Polycrystalline Solar Power Modules

Gällivare PhotoVoltaic

We connect you to the sun

SwedModule's on Linköping's public library. The system is installed by Switchpower.

TOP SWEDISH QUALITY

Swedish technology you can trust is one of the cornerstones in Gällivare PhotoVoltaic's philosophy. The SwedModule product range is produced using only high quality raw materials from leading suppliers. The SwedModule is ideal for individual houses or buildings, on facades or rooftops but also for large scale solar power systems.

DESIGN OF THE SWEDMODULE

The cells are encased in high transmission low-iron tempered glass, multi-layers of ethylene vinyl acetate (EVA) as well as Tedlar film. This provides the modules with top-quality protection against external environmental effects. GPV's Solar Power Modules also have bypass diodes to minimise power loss in case of shading and protect against hot spot effect.

QUALITY CONTROL

During the production process the modules pass through several quality control check points and they are carefully checked and tested prior to delivery. The final test takes place in a solar simulator, where the modules are tested under Standard Test Conditions (STC 1000W/m²). Every modules serial number and its test data are stored in our database.

FLEXIBILITY

We have the advantage to have a flexible production facility where we strive to meet our customer's needs. Choose from white, black or transparent tedlar. Silver or black frame or no frame at all. Please contact us for more information and ask for a quotation for a product especially designed for you.

WARRANTY

GPV offer a product guarantee of 10 years and a 25 year performance guarantee for an 80 % power output on all standard products.

In order to further guarantee the quality of our products we are certified in accordance with:

- EN IEC 61215 (design qualification and type approval)
- EN IEC 61730 (safety qualification)
- IEC 61701 (salt mist corrosion test)
- SS-EN ISO 9001:2000 (Quality Management System)
- SS-EN ISO 14001:2004 (Environmental Management System)

SWEDMODULE GPV200-GPV230

Polycrystalline Solar Power Modules

CONSTRUCTION FRONT TO BACK

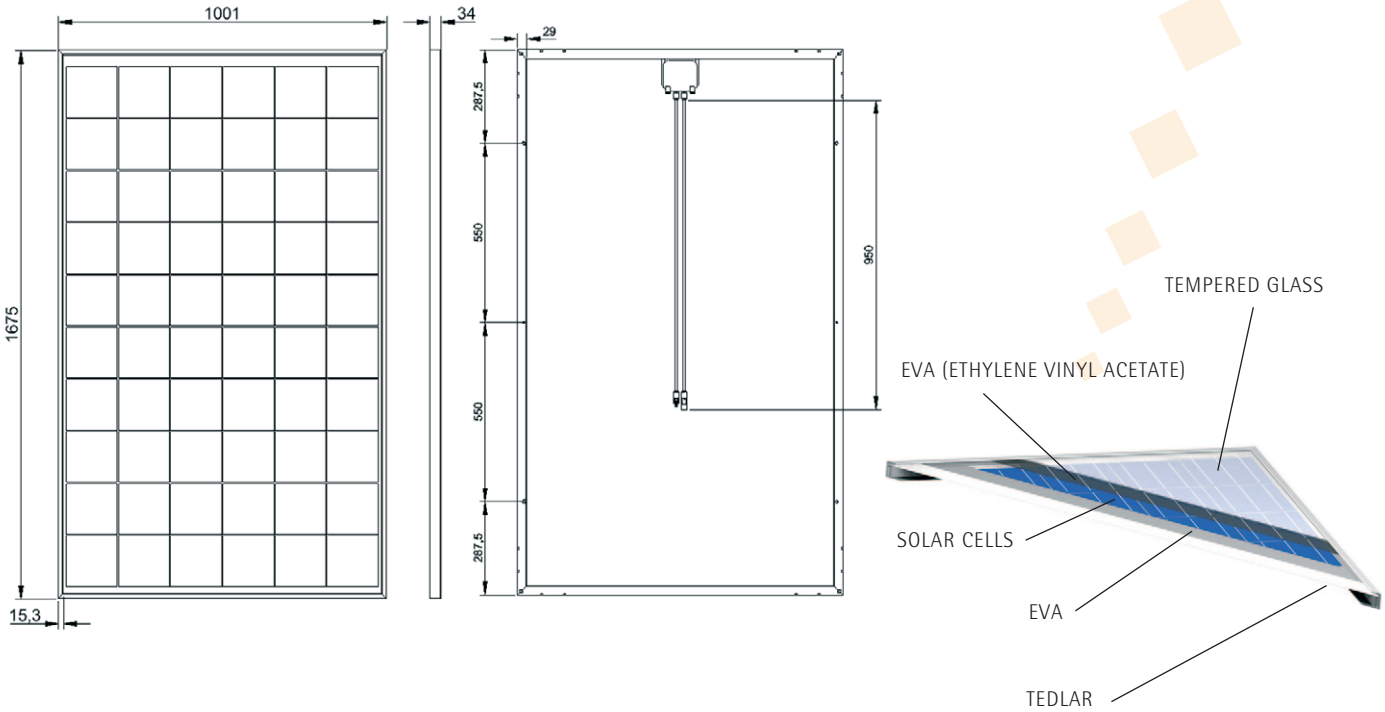

POWER SPECIFICATIONS

Performance under standard test conditions

1000 W/m², 25°C, 1.5 AM

	GPV200	GPV205	GPV210	GPV215	GPV220	GPV225	GPV230
Average max. power (P_{max})	203.3 Wp	207.2 Wp	212.6 Wp	217.4 Wp	222.7 Wp	226.2 Wp	233.5 Wp
Open circuit voltage (V_{oc})	36.6 V	36.6 V	36.7 V	36.8 V	36.8 V	36.8 V	36.8 V
Max. power voltage (V_{mpp})	29.0 V	29.1 V	29.2 V	29.3 V	29.3 V	29.3 V	29.3 V
Short circuit current (I_{sc})	7.58 A	7.67 A	7.84 A	7.97 A	8.13 A	8.25 A	8.51 A
Max. power current (I_{mpp})	7.01 A	7.12 A	7.28 A	7.42 A	7.60 A	7.72 A	7.97 A
Module efficiency	12,1%	12,4%	12,7%	13,0%	13,3%	13,5%	13,9 %

Performance at

800W/m², NOCT, AM1.5

	GPV200	GPV205	GPV210	GPV215	GPV220	GPV225	GPV230
Average max. power (P_{max})	145.4 Wp	148.1 Wp	152.0 Wp	155.4 Wp	159.2 Wp	161.7 Wp	166.9 Wp
Open circuit voltage (V_{oc})	33.1 V	33.1 V	33.2 V	33.3 V	33.3 V	33.3 V	33.3 V
Max. power voltage (V_{mpp})	26.0 V	26.1 V	26.2 V	26.3 V	26.3 V	26.3 V	26.3 V
Short circuit current (I_{sc})	6.26 A	6.34 A	6.48 A	6.59 A	6.72 A	6.82 A	7.03 A
Max. power current (I_{mpp})	5.59 A	5.68 A	5.81 A	5.92 A	6.06 A	6.16 A	6.36 A

All values with a tolerance of ±3 %

Minor reduction in efficiency under partial load conditions at 25°C: at 200W/m², 95% (± 3 %) of the STC efficiency (1000 W/m²) is achieved.

THERMAL CHARACTERISTICS

NOCT	46°C
TC I_{sc}	0.034 %/K
TC V_{oc}	-0.34 %/K

SYSTEM INTEGRATION PARAMETERS

Maximum system voltage: SC II 1000 V_{DC}

Maximum reverse current: Do not apply external voltages larger than V_{OC} to the module

Gällivare PhotoVoltaic AB reserves the right to make specification changes without prior notice. Please contact your nearest stockist/distributor or visit our website to obtain the latest specification sheet.

PHYSICAL SPECIFICATIONS

Cell type	Polycrystalline
Cell dimension (+/- 0,5mm)	156mm x 156mm
Cells per module	60
Module weight	22 kg
Module size (+/- 2mm) (L x H x W)	1675 mm x 1001 mm x 34 mm
Frame	Anodized aluminium

Gällivare PhotoVoltaic AB Företagscentrum, Box 840, SE-982 28 Gällivare, Sweden

T +46 970 158 30 F +46 970 158 98 info@gpv-solar.com www.gpv-solar.com

GPV - A MEMBER OF THE BOREVIND GROUP

Gällivare PhotoVoltaic

ASI THRU® thin-film solar module, semitransparent

ASITHRU-30-SG semitransparent 36 V_{DC}

- More energy
- General approval for use in overhead glass construction
- Favorable price per units of surface area
- Multi-purpose module

Frameless ASIOPAK-30-SG modules are ideally suited for installation in standard facades and roof profile systems.

Module type key:
SG = laminated safety glass

The structural characteristics of the glass module meet nearly all of the installation requirements specified in DIN 1055. In order to ensure compliance with guide-lines for overhead glass construction, PVB is used as a laminating foil. A general approval for use in overhead glass construction has been issued by the Deutsches Institut für Bautechnik (DIBt-the German Institute of Architectural Engineering).

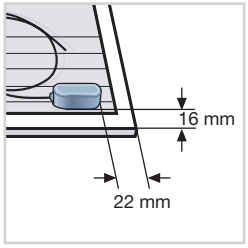

Lateral mounting clearance from the connection button

MC®-plug connectors

The modules are factory equipped with plug connectors and can be connected quickly and safely in series.
The specific characteristics of ASI THRU® solar modules eliminate the need for bypass diodes.

ASITRHU-30-SG solar modules are designed on the basis of silicium thin-film technology as ASI® tandem cells on a glass substrate.
The frameless ASI THRU® solar module consists of a glass front pane with ASI® tandem cells, PVB foil and a heat strengthened backing glass.
ASI THRU® solar modules demonstrably produce maximum energy yields. ASI THRU® solar modules combine the features of solar electricity generation, shadowing glare reduction, transparency and sound glass construction in a single element.

New solar architecture: brilliant, colorless transparency

RWE SCHOTT Solar

Electrical data

Initial nominal power		33 Wp
Nominal power*	P_{nom}	27 Wp
Voltage at maximum-power point*	U_{mpp}	36 V
Current at maximum-power point*	I_{mpp}	0.75 A
Short-circuit current*	I_{sc}	1.02 A
Open-circuit voltage*	U_{oc}	49 V

The quoted figures are subject to a production tolerance of ± 10%.

*** These data represent stabilized electrical module performance at standart test conditions (STC – 1000 W/m², spectrum AM 1.5, 25 °C cell temperature). The nominal power may be initially approx. 18% higher than the quoted stabilized power data.**

Dimensions and weights

Dimensions	1000 x 600 mm²
Module glass thickness / module thickness with connection button	10 mm / 22 mm
Four-sided non-photoactive margin for clamp mounting	16 mm
Weight	14 kg

Characteristic data

Solar cell type	thin-film amorphous silicon in ASI® tandem cells
Appearance	uniformly dark-brown
Semitransparency	about 10 % transmission, colour-neutral
Electrical connection	double insulated cable (Huber & Suhner), 2.5 mm² cross-section, 100 cm length per polarity, MC®-plug connectors

Cell temperature coefficients

Referred to nominal power	T_K (P_n)	- 0.2 % / K
Referred to open-circuit voltage	T_K (U_{oc})	- 0.33 % / K
Referred to short-circuit current	T_K (I_{sc})	+ 0.08 % / K
The temperature dependence of the power output is particularly low for ASI THRU®-solar modules.		

Limits

Maximum system voltage	1000 V_{DC}
Temperature arrange	- 40 °C... + 85 °C
Maximum surface load	• two-sided clamping along length: 3200 N/m² • four-sided clamping: 4600 N/m²

Specifications subject to change without notice.

Qualification	IEC 61646 certified
	CE conformity
	Safety Class II

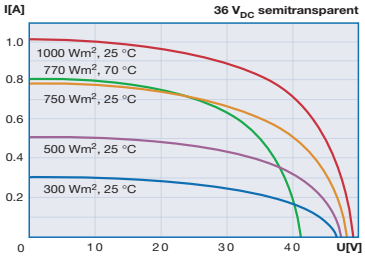

Current/voltage characteristics at different solar irradiation levels and module temperatures.

RWE SCHOTT Solar GmbH
Hermann-Oberth-Str. 11
85640 Putzbrunn, Germany
P +49 (0) 89 / 4 62 64 - 100
F +49 (0) 89 / 4 62 64 - 111
E phototronics-sales@rweschottsolar.com
I www.rweschottsolar.com

RWE SCHOTT Solar